PMayA20

Lateral torsional buckling of partially restrained beams of S690 welded I-sections

Kai Wang[1,2], Meng Xiao[1,2], Kwok-Fai Chung[1,2*], and David A. Nethercot[1,2,3]

[1]*Department of Civil and Environmental Engineering,*

The Hong Kong Polytechnic University, Hong Kong SAR, China.

[2] *Chinese National Engineering Research Centre for Steel Construction (Hong Kong Branch)*

The Hong Kong Polytechnic University, Hong Kong SAR, China.

[3] *Department of Civil and Environmental Engineering, Imperial College London, U.K.*

* *Corresponding author: kwok-fai.chung@polyu.edu.hk*

Abstract

This paper reports a systematic experimental investigation into the structural behaviour of a total of eighteen simply supported beams of high strength S690 welded I-sections with various restraint conditions, focussing on lateral torsional buckling. Deformation characteristics of these beams, critical failure modes and moment resistances, are fully presented and discussed. In general, these beams of S690 welded I-sections were found to behave in an essentially similar manner to beams of S355 I-sections. Lateral torsional buckling in these beams was thoroughly assessed and compared with the predictions of EN1993-1-1 using their non-dimensionalized slenderness, determined using the procedures of EN 1993-1-1, and measured mechanical properties, geometrical dimensions and restraint conditions. It was demonstrated that the codified design rules were very conservative when being extended to cover these beams of S690 welded I-sections.

This comprehensive experimental investigation provides scientific evidence and test data that highlights a need to improve structural efficiency of the design rules in EN 1993-1-1 so that structural engineers can fully exploit the structural benefits offered by these high strength S690 steels in construction.

Keywords:

High strength steels; Lateral torsional buckling; Welded sections; Partially restrained beams; Non-dimensionalized slenderness.

1. Introduction

Nowadays, the term 'high strength steels' is commonly taken to mean steel plates with yield strengths equal to or larger than 690 N/mm2; they are manufactured to EN 10025: Part 6 [1]. When compared with the more commonly used structural steels with yield strengths of 355 N/mm2, the high strength steels are able to offer 90 to 100 % increase in resistances with a premium of an additional cost of about 25 to 35%. Hence, many engineers believe that the wide adoption of these S690 steels will have a huge impact on the Construction Industry worldwide as self-weights of structural members, in particular, heavily loaded columns, will be significantly reduced [2]. However, they are less ready to use these S690 steels as heavily loaded beams as these beams may be controlled by deflection rather than strength in design. However, experienced steel designers are often able to counter this problem by introducing pre-cambers into these beams during fabrication. Hence, high strength S690 welded I-sections are highly effective structural members for carrying heavy loads over their spans, and it is important to examine their structural behaviour through experiments on beams with various restraint conditions against lateral torsional buckling.

1.1 Lateral torsional buckling of beams

Lateral torsional buckling, or torsional flexural buckling, in unrestrained beams is an important aspect of structural behaviour in steel structures [3, 4], and there were many experimental, analytical and numerical investigations conducted by many researchers over the past fifty years. Hence, an attempt was made to summarize those essential developments on experimental, analytical and numerical investigations which led to widely adopted methods in modern design recommendations and codes of practice.

In the 1960's, when there was comparatively little known about this phenomenon, many investigators carried out small as well as full scale experiments on long unrestrained beams to examine this form of structural instability [5, 6, 7, 8, 9]. Similar to the use of a slenderness, λ, in column design, an equivalent slenderness, λ_{LT}, was developed to be used in beam design. It became very important when assessing the effectiveness of various positional and directional (rotational) restraints to both the loaded points and the supports of the beams as these restraints defined effective lengths of the beams, L_e, undergoing lateral torsional buckling [10]. The presence of residual stresses in both hot-rolled and welded sections always caused early yielding in their cross-sections, and hence, a significant reduction in their flexural rigidities. Both initial out-of-straightness and twists often imposed adverse effects on the

structural behaviour of these beams, especially in I-sections, leading to significant reductions in their member resistances. It should be noted that lateral torsional buckling behaviour in Grade 55 hot rolled I-sections was examined experimentally for comparison with those of Grade 43 hot rolled I-sections in the late 1960s [11]. The effects of increased yield strengths on lateral torsional buckling of these beams were assessed. In general, the buckling behaviour of these two types of beams was found to be similar in many ways, and there were significant increases in the buckling moment resistances due to an increase in the yield strengths. Moreover, the effects of strain hardening on the moment resistances of fully restrained steel beams [12] were examined systematically in tests, and the measured moment resistances of these beams were found to be significantly larger than their design moment resistances based on measured dimensions and yield strengths. Hence, contributions of strain hardening beyond yielding in these beams should be quantified, whenever feasible. In the 1980's, experimental investigations on long span castellated beams with multi web openings were reported, and their structural behaviour was demonstrated [13] to be very similar to those beams without web openings though section properties of the perforated cross-sections should be adopted in design.

Moreover, a large number of analytical formulations were proposed [14, 15, 16] to allow for variations of the bending moments between restraints in the beams through a parameter which was commonly referred as an equivalent moment uniform factor, m . It should be noted that in the 1980's, only limited analytical solutions for the elastic critical moments, M_{cr} , of beams under a few simple loading and support conditions were available - although this situation did change once Finite Element solutions became available. In order to have test results readily analysed, many experiments were conducted with specially devised loading and support attachments to match with both the loading and the support conditions of those analytical solutions. The effects due to heights of load application points above the centroids of the beam sections were also examined as additional twisting moments might be induced onto the beams during buckling, i.e. a "de-stabilizing" condition. Moreover, mono-symmetric I-sections were widely used in supporting over-head cranes in many industrial buildings, and a mono-symmetric parameter, β_x , was developed [17] for accurate prediction of their buckling behaviour.

In the 1980s, efficient beam elements with a total of 7 degrees of freedom (DoF), i.e. 3 translational DoF, 3 rotational DoF and 1 warping DoF, were developed to assess lateral torsional buckling of open sections, such as I-sections as well as T- and L-stiffeners. Moreover, various shell elements became readily available [18] to deal with general strength and buckling behaviour of these beams which cross-sections were made up thick as well as thin plates. These shell elements were able to simulate lateral torsional buckling, local plate buckling and distortional buckling as well as their interactions in the beams. They were also able to simulate a wide range of loading as well as support conditions of these beams both in experiments and in practice, and both material and geometrical non-linear analyses were readily available to simulate the entire load-deformation characteristics of these beams.

In EN 1993-1-1 [19], design for both axial buckling of columns and lateral torsional buckling of beams were harmonized using the same buckling formulation, and both the non-dimensionalized slenderness for columns, $\overline{\lambda}$, and the non-dimensionalized slenderness $\overline{\lambda}_{LT}$ for beams were adopted to assess their member resistances through the use of the same set of member buckling curves. Both $\overline{\lambda}$ and $\overline{\lambda}_{LT}$ were defined respectively in Cl. 6.2.2 and 6.3.2 as follows:

$$\overline{\lambda} = \sqrt{\frac{Af_y}{N_{cr}}} \quad ; \quad \overline{\lambda}_{LT} = \sqrt{\frac{W_y f_y}{M_{cr}}} \qquad (1)$$

where

f_y is the design strength of the section;

A is the cross-sectional area of the section;

W_y is the elastic or the plastic section modulus of the section;

N_{cr} is the critical buckling load of the column; and

M_{cr} is the elastic critical buckling moment of the beam.

It should be noted that both $\overline{\lambda}$ and $\overline{\lambda}_{LT}$ were formulated in terms of member resistances rather than geometric properties of the columns and the beams. For $\overline{\lambda}_{LT}$, the values of M_{cr} were readily obtained through various design expressions [14, 15, 16] or eigenvalue analyses using linear elastic finite element models.

1.2 Previous research works on high strength steel in construction by the authors

In order to promote the effective use of high strength steels in construction, an extensive research programme into mechanical properties and structural behaviour of high strength S690 welded sections was conducted by the authors; key research areas include:

a) microstructural changes in S690-QT steels due to heating / cooling cycles during welding [20];
b) reductions in mechanical properties of S690-QT welded sections with various heat input energy during welding [21];
c) numerical simulation of welding, and prediction of welding-induced residual stresses in S690 welded H-sections through heat transfer and thermomechanical analyses [22];
d) structural behaviour of stocky and slender columns of S690 welded H-sections under i) compression [23], and ii) combined compression and bending [24];
e) numerical simulation of i) transverse bending, and ii) longitudinal welding, and prediction of residual stresses in S690 structural hollow sections with various internal radii [25];
f) structural behaviour of T-joints between S690-QT cold-formed circular hollow sections [26] under i) brace axial compression, and ii) brace in-plane moments.

In general, although the maximum values of welding-induced residual stresses in these S690 welded H-sections were found to be larger than those in S355 welded H-sections of similar sizes with similar welding processes because of increased yield strengths, their effects on the structural behaviour of these S690 welded H-sections were found to be proportionally less pronounced [22] when compared with those welded sections of S355 steels. It should be noted that in a recent experimental investigation conducted by the authors, a series of slender columns of S690 welded H-sections were tested to examine their structural behaviour under axial compression. It was demonstrated that axial buckling behaviour of these welded H-sections was very similar to those slender columns of S235 and S355 welded H-sections [23], and interaction between material yielding and member buckling was readily assessed with the member slenderness of the columns. Hence, it was proposed to extend applicability of the design rules given in EN 1993-1-1 to cover axial buckling of these slender columns of S690 welded H-sections. Based on the test results obtained in the experiments, the current design rules were shown to provide close and yet conservative predictions of the measured resistances of these columns when appropriate values of the controlling design parameters were selected.

Consequently, it is highly desirable to examine the structural behaviour of partially restrained beams of S690 welded I-sections against lateral torsional buckling so as to check the applicability of the design rules in EN 1993-1-1 to these beams.

1.3 Objectives

In order to promote the effective use of high strength steels in construction, it was important to examine lateral torsional buckling of partially restrained beams of high strength S690 welded I-sections under various restraint conditions. A comprehensive experimental investigation into the structural behaviour of three different test series of simply supported beams was conducted, and in each series, there were six welded I-sections with different cross-sectional dimensions, namely, Sections HSB1 to HSB6, as shown in Figure 1. While all these beams were tested under single point loads, there were three different restraint and support conditions, as shown in Figure 2, in these test series as follows:

- Series SA: A total of six simply supported beams with two lateral restraints and two end supports
- Series SB: A total of six simply supported beams with *only one* lateral restraint and two end supports
- Series SC: A total of six simply supported beams with *only one* lateral restraint together with *one* end support and *one* modified end support

By specifying different shear spans and providing three different combinations of lateral restraint conditions in these three series of beams, a wide range of structural behaviour on lateral torsional buckling in these beams was readily tested for direct comparison. Extensive instrumentation was provided so as to capture various deformation characteristics of the beams, in particular, load-deflection curves, failure modes and moment resistances. Key results of these tests were fully presented and compared. As these sections were fabricated with 6, 10 and 16 mm thick S690 steel plates, standard tensile tests on coupons cut from these steel plates were conducted to obtain their mechanical properties as reference data for subsequent analyses.

The measured moment resistances of these beams were thoroughly assessed and compared according to the design rules given in EN 1993-1-1 [19] based on measured mechanical properties, geometrical dimensions and restraint conditions. More specifically, for those effectively fully restrained beams in Series SA, their cross-section moment resistances, $M_{c,Rd}$, were expected to be readily mobilized, and these test results were therefore employed to check whether the current rules of section classifications were applicable to these S690 welded I-sections. For those partially restrained beams in Series SB and SC, lateral torsional buckling was expected to be critical, and the corresponding buckling moment resistances, $M_{b,Rd}$, were determined according to the non-dimensionalized slenderness $\overline{\lambda}_{LT}$. Hence, through linear elastic finite element models, the elastic critical moment resistances of these beams, M_{cr}, corresponding to their specific restraint conditions, were obtained to determine $\overline{\lambda}_{LT}$. It was essential to verify whether the current design rules, which were developed for S235 to S460 steels, were equally applicable to design of these S690 welded I-sections against lateral torsional buckling.

In the present investigation, the areas of interest were

- mechanical properties of the S690 steel plates with various thicknesses;
- local plate buckling in the beams of S690 welded I-sections in Series SA;
- lateral torsional buckling in the beams of S690 welded I-sections in Series SB and SC with various restraint conditions;
- applicability of current design rules in EN 1993 [19, 29]:
  i) Cl. 5.5 Classification of cross-sections, and
  ii) Cl. 6.3.2 Buckling resistances of members;
- effects of reduced restraints onto those beams in Series SC, when compared with those in Series SB.

1.4 Standard coupon tests on S690 steel materials

According to BS EN ISO 6892-1 [27], standard tensile tests were conducted to determine the stress-strain characteristics of the S690 steel plates. A total of 12 standard cylindrical coupons with circular cross-sections were tested as a total of three S690 steel plates of different thicknesses, namely, 6, 10 and 16 mm, were utilized to fabricate welded I-sections. Dimensions of these coupons are shown in Figure 3a). It should be noted that through the use of an extensometer with a gauge length of 25 mm, all these tensile tests were conducted

through the application of elongations onto the coupons with precision measurements. In order to obtain the full deformation ranges of these coupons, a high resolution digital camera was used, as shown in Figure 3b), to take digital images of these coupons at specific time intervals throughout the tests. After counting the numbers of pixels for covering the lengths of the coupons in these images, their elongations were readily obtained [21, 28]. Typical measured stress-strain curves of these coupons were plotted in Figure 3c) while their key mechanical properties are summarized in Table 1.

It should be noted that the relevant requirements on the mechanical properties of S690 steels given in EN 1993-1-1 [19] and EN 1993-1-12 [29] are:

i) $f_u / f_y \geq 1.05$; 2a)

ii) $\varepsilon_L \geq 10\ \%$; and 2b)

iii) $\varepsilon_u \geq 15\ \varepsilon_y$ 2c)

Comparing these measured mechanical properties with various criteria given above, it is shown that these steels generally meet the requirements for structural design. Therefore, it is evident that properly produced S690 steels are directly applicable in steel construction according to EN 1993-1.

1.5 Fabrication of S690 welded I-sections and welding-induced residual stresses

All the S690 welded I-sections were fabricated in an established steelwork fabricator. In order to minimize or even to eliminate adverse heating effects onto the S690 steel plates during fabrication, they were carefully flame-cut into plates of specific dimensions. These plates were then welded together to form I-sections by a qualified welder using a gas metal arch welding (GMAW) method, as shown in Figure 4. It should be noted that a matching welding electrode of GM110 [30] was adopted in the fillet-welding of these sections. Based on experiences in previous research projects on S690 welded H-sections [20, 21], the following set of optimized welding parameters were adopted:

- Welding voltage: 28 V
- Welding current: 225 A
- Welding speed: 5 mm/s, and
- Efficiency factor η for GMAW: 0.85

Based on these welding parameters, the heat input energy was found to vary between 1.0 and 1.3 kJ/mm during welding, as shown in Table 2. Hence, any welding effects on the mechanical properties of these S690 welded I-sections at their welded junctions were kept to be minimal [22].

In order to assess the effects of welding-induced residual stresses in these S690 welded I-sections, the hole drilling method to ASTM E837 [31] was employed to measure surface residual stresses in the outer surfaces of both the top and the bottom flanges as well as the webs of these I-sections [22, 32]. After careful execution and data analyses, Figure 5 gives plotted typical residual stresses obtained from Sections HSB2, HSB4 and HSB6. It should be noted that these measured stresses were found to be significantly smaller than anticipated [33], because of the use of multi-pass welding. These findings were consistent with similar measurements conducted by the authors on S690 welded H-sections [22, 23, 25]. Refer to Reference 32 for details.

2 Experimental investigation

Three test series, namely, Series SA, SB and SC, were conducted with a total of eighteen simply supported beams of the S690 welded I-sections under single point loads [32]; the test programmes are summarized in Tables 3, 4 and 5 respectively. It should be noted that:

- Series SA

  Six beam tests on various S690 welded I-sections were conducted under single point loads using different shear spans, L_a , with two lateral restraints, i.e. Restraints R1 and R2, and two end supports in each test, i.e. Supports Q and S, as shown in Figure 2a). These beams were considered to be restrained laterally so that the full moment resistances of these I-sections were readily mobilized. It should be noted that local buckling in the plate elements of these sections was expected to take place after yielding, and these results were used to verify applicability of the current design rules on section classification when being extended to these S690 welded I-sections.

- Series SB

  Another six beam tests on various S690 welded I-sections were conducted under single point loads of different shear spans, L_b , with only one lateral restraint, i.e. Restraint R1,

and two end supports, i.e. Supports Q and S, in each test, as shown in Figure 2b). These beams were considered to be partially restrained, and their cross-sectional moment resistances were unlikely to be fully mobilized. Hence, these beams were expected to undergo lateral torsional buckling between Restraint R1 and Support S.

- Series SC

  In order to further examine lateral torsional buckling of these S690 welded I-sections, another six beam tests on various S690 welded I-sections were conducted with a similar provision of lateral and end restraints adopted in Series SB, but with a modified end restraint in Support S. Hence, these beams were under single point loads of different shear spans, L_c , with a lateral restraint, i.e. Restraint R1, an end support, i.e. Support Q, and a modified end support, i.e. Support S, as shown in Figure 2c). The modified end support was readily achieved by removal of web stiffeners in both sides of the webs of the beam ends. Hence, these beams were expected to become highly susceptible to lateral torsional buckling between Restraint R1 and Support S.

The measured cross-sectional dimensions of these welded I-sections are also summarized in Tables 3, 4 and 5. By extending the design rules given in Cl. 5.5 Classification of cross-sections of EN 1993-1-1, Sections HSB1 to HSB3 were classified as Class 1, 2 and 3 sections respectively while Section HSB4 was classified as a Class 2 section. It should be noted that both Sections HSB5 and HSB6 were mono-symmetrical I-sections, and they were classified as Effective Class 2 sections.

Hence, a total of six S690 welded I-sections with different cross-sectional dimensions and section classifications were included in the experimental investigation, and lateral torsional buckling of these beams with various practical restraints was examined systematically.

2.1 Test set-up, instrumentation and procedures

A typical test set-up for a simply supported beam adopted in this experimental investigation is shown in Figure 6a). A hydraulic jack with a 2,000 kN capacity was installed in the loading frame to conduct the test while the applied load was measured by a load cell with a 1,500 kN capacity. It should be noted that the load was applied to the top flange of the beam at the point of load application. Support Q was a roller while Support S was a pinned support, and both the reaction forces were applied to the bottom flange of the beam at both beam ends.

In order to prevent any out-of-plane displacement of the beam at the point of lateral restraint, a stiff lateral restraint system was designed, as shown in Figure 6b). It should be noted that

i) Two T-sections were welded onto both sides of the web of the beam at the location of each lateral restraint.
ii) The flanges of these T-sections were held in position by a pair of channel sections which were fixed onto a strong support.
iii) Teflon membranes were attached onto the contact surfaces between both the T-sections and the channel sections with greases in order to minimize any friction.

Hence, the beam was only allowed to move vertically without any lateral nor torsional displacement at the location of each lateral restraint.

In each test, when the test beam was installed onto the testing frame, both the end supports were carefully adjusted to receive the beam ends. Initial out-of-straightness of the beam in both the Y- and the Z- planes was then measured and recorded. The loading attachment was carefully positioned onto the beam, and it was aligned as far as practicably possible to minimize any undesirable effects on the beam due to misalignment. In general, owing to the high quality of steel fabrication, the out-of-straightness of these beams were found to be typically smaller than 2.0 mm though the fabrication tolerance specified was L/1000, i.e. 2.25 to 4.5 mm.

All these tests were conducted with extensive instrumentation to capture the load-deformation characteristic of these beams, as illustrated in Figure 7:

i) up to 8 linear displacement transducers, namely, LVDTs 01 to 08, were installed to measure
   - vertical displacements, Δ_z , at the loaded points of the beam,
   - rotations, θ_y , at both ends of the beam, and
   - lateral displacements, δ_y , of the beam for monitoring.

ii) a maximum of 8 strain gauges, namely, SG1 to SG8, were mounted onto a cross-section 100 mm from the loaded points, and these strain gauges were used to measure:
   - direct strains across the depth of the section under bending.

The following loading procedure was adopted in each of the tests:

a) Before testing, a pre-loading process was performed. A force of 30% of the predicted failure load of the beam was applied. Then, the force was reduced at a rate of 50 to 75 kN per minute. This process was repeated three times to minimize initial bedding.

b) In the initial stage of testing, the force was applied at a rate of 20 to 40 kN per minute, and it was steadily increased up to 80% of the predicted failure load.

c) Then, the force was applied through monitoring of a vertical displacement, Δ_z , and an increase in the displacement at a rate of 1.0 to 2.0 mm per minute was imposed steadily until apparent unloading; the peak load was recorded as the measured failure load of the beam, N_{Rt} .

d) Finally, additional vertical displacement Δ_z was imposed at a rate of 2.0 to 4.0 mm per minute, and the test was terminated when the value of the applied force was found to drop below 80% of the peak load.

2.2 Test results for Series SA

All the tests in this Series except Section HSB6 were successfully completed. All the measured cross-sectional dimensions of these Sections as well as key data and results of these tests were summarized in Table 3. Details of the test results were described in the following.

2.2.1 Load deformation characteristics

All the measured applied moment-deformation curves of the beams in Series SA are plotted in Figure 8. In each test, the vertical deflection at the loaded point, Δ_z , was taken as the average of the readings measured with LVDTs 3 and 4 while the end rotation of the beam, θ_y , was determined according to the difference of the readings measured with LVDTs 1 and 2.

In general, all the applied moment - vertical deflection (M - Δ_z) curves were linear up to 80% to 90% of the predicted resistances, and they became non-linear only when approaching the peak loads of the beams. After significant deformations and yielding in the cross-sections of the beams, unloading in the curves became apparent. Similar observations were also found in the applied moment - end rotation (M - θ_y) curves of the beams.

2.2.2 Failure modes

All the beams were shown to fail under moments with significant vertical displacements, and hence, gross deformations under the applied loads. Significant local buckling in both the top (compression) flanges and the webs of all these beams was apparent, as shown in Figure 9.

It should be noted that careful observations on these beams during the tests as well as detailed inspection on regions of significant deformations in these beams after the tests were made, and no weld fracture was found in any part of these beams.

2.2.3 Moment resistances of welded I-sections

The measured failure loads, N_{Rt} , and the corresponding moment resistances, M_{Rt} , of the beams are presented in Table 3b). The cross-sectional moment resistances of these beams, $M_{c,Rd}$, which were determined with measured dimensions and yield strengths, were also provided for comparison. According to the load-deformation curves as shown in Figure 8, the following findings are evident:

- Sections HSB1 and HSB2 were classified as Class 1 and 2 sections, and their plastic moment resistances were readily mobilized. Section HSB3 was classified as Class 3 sections, and only its elastic moment resistance was readily mobilized. Hence, the current design rules were applicable to all these three Sections.

- Sections HSB4 were classified as Class 2 while Sections HSB5 and HSB6 were classified as Effective Class 2 sections respectively, and it was evident that their plastic moment resistances were readily mobilized. Hence, the current design rules were shown to be applicable to these three Sections.

2.3 Test results for Series SB and SC

All the tests in these two Series were successfully completed. All the measured cross-sectional dimensions of these Sections as well as key data and results of these tests are summarized in Tables 4 and 5 respectively. Details of the test results are described in the following.

2.3.1 Load deformation characteristics

All the measured applied load deformation curves of the beams in Series SB and SC are plotted in Figures 10 and 11 respectively. In each test, the vertical deflection at the loaded point, Δ_z , was taken as the average of the readings measured with LVDTs 3 and 4 while the lateral displacements of the beams, δ_y , taken as the readings measured with LVDT 5 at specific locations of the beams are also provided. In general, all the applied moment – vertical deflection (M - Δ_z) curves were linear up to 80% to 90% of the predicted resistances, only becoming non-linear when approaching the peak loads of the beams. An inspection on the applied load-lateral displacement (N - δ_y) curves of these beams showed a clear onset of lateral torsional buckling of these beams.

2.3.2 Failure modes

Typical modes of failure in these beams of the two Series were illustrated in Figure 12. It was found that

Series SB: Lateral torsional buckling in beams

- According to the observed deformed shapes and measured data, lateral torsional buckling was evident in all the beams in the Series, and it took place between Restraint R1 and Support S in these beams. Both Figures 12a) and b) illustrate typical deformed shapes of the beams undergoing lateral torsional buckling, and lateral displacements of the top (compression) flanges of the beams together with longitudinal twisting were apparent.

Series SC: Lateral torsional buckling in beams with apparent distortion at Support S

- As shown in Figures 12c) and d), lateral torsional buckling was evident in all the beams in the Series, and it took place between Restraint R1 and Support S in these beams together with significant cross-sectional distortion at Support S due to an absence of vertical web stiffeners. Hence, the unstiffened webs were unable to provide effective restraints to the top flanges of the beams, and cross-sectional distortions in these beams at the end supports

were apparent. Consequently, the effective lengths of these beams were significantly increased.

2.3.3 Member resistances of welded I-sections

The measured failure loads, N_{Rt} , and the corresponding member resistances, $M_{b,Rt}$, of the beams in Series SB and SC were presented in Tables 4b) and 5b) respectively. The moment resistances of these beams, $M_{c,Rd}$, which were determined with measured dimensions and yield strengths, were also provided for comparison. Refer to Section 4 for assessment on these member resistances.

Nevertheless, it should be noted that the ratios M_{Rt} / $M_{c,Rd}$ of some of the beams in both Series SB and SC were found to be larger than 1.0. Hence, despite of the occurrence of lateral torsional buckling, the moment resistances of some of these beams were fully mobilized.

2.4 Measured direct strains within the cross-sections

A total of 8 strain gauges, namely SG1 to SG8, were used to measure direct strains at a specific cross-section in each of the beams in these Series, as shown in Figure 7. All the measured strain data for all the beams at failure in Series SA, SB and SC were plotted in Figures 13, 14 and 15 respectively. It should be noted that

- Series SA

  For most of the welded I-sections in this series, the strain distributions within the cross-sections of the beams followed typical strain distributions under bending, i.e. the top flanges were under uniform compression stresses and the bottom flanges were under uniform tension stresses while the webs were under linearly varying stresses, as shown in Figure 13. It should be noted that owing to occurrence of local plate buckling in the top flanges in some beams, non-uniform compression stresses are also obtained.

- Series SB and SC

  In the welded I-sections in these two series, the strain distributions within the cross-sections of the beams followed typical strain distributions under bending and warping actions, i.e. while the webs were under linearly varying stresses, the top flanges were under non-uniform compression stresses and the bottom flanges were under non-uniform tension stresses, as shown in Figures 14 and 15. These non-uniform compression and tension

stresses in the top and the bottom flanges were direct results of bi-moments due to lateral torsional buckling.

3 Finite Element Modelling

In order to determine the values of the elastic critical moment resistances, M_{cr} , of all the beams of S690 welded I-sections in Series SA, SB and SC through eigenvalue analyses, finite element models of Sections HSB1 to HSB6 were established with the general finite element package ABAQUS (Version 6.14) [34]. It should be noted that the flanges and the webs of the welded I-sections together with the web stiffeners at beam ends were modelled with shell elements S4R, as shown in Figure 16. Both the loading and the support conditions of the beams in the various series were carefully modelled with appropriate definitions of various degrees of freedom at suitably selected element nodes of the models. Measured dimensions of the beams were used in all the models. Figure 16 also illustrates typical models of the beams in the various series. It should be noted that in order to model the stiff lateral restraining systems provided to these beams, a total of four nodes at the top flange as well as another four nodes at the bottom flange of the beams in the regions of the stiff lateral restraining systems were assigned to be fixed in the lateral direction only. Hence, the restraint conditions of these beams in the tests were adequately modelled in these models.

3.1 Elastic critical moment resistances

After completion of linear elastic analyses on the models, a multiple eigenvalue analysis was conducted to determine the lowest 5 to 10 eigenvalues of each of these beams, depending on various geometric ratios of the flanges and the webs in these beams. Owing to possible local plate buckling in both the flanges and the webs as well as their interactions, the eigenmodes corresponding to the lowest eigenvalues might not relate to lateral torsional buckling of the beams, and hence, it was necessary to identify the appropriate eigenmodes, and adopt the corresponding eigenvalues for determination of the elastic critical moment resistances M_{cr} of these beams. Figure 16 illustrates typical eigenmodes of these beams in Series SA, SB and SC with different restraint conditions together with corresponding values of M_{cr} .

In general, it should be noted that:

- All the beams in Series A were found to buckle with local plate buckling in their flanges and webs between lateral restraints, and the values of M_{cr} were found to be significantly larger than their section resistances under bending.

- For those beams in Series B and C, the buckled mode shapes of the beams in Series C were found to be very different, i.e. more slender, when compared to those of the beams in Series B, owing to an absence of the web stiffeners at Support S.

All the values of Mcr of the beams in Series SA, SB and SC are summarized in Tables 3b), 4b) and 5b) respectively, and hence, the corresponding non-dimensionalized slendernesses, $\overline{\lambda}_{LT}$, of these beams are obtained for subsequent data analyses.

4 Section and member resistances under bending

It was important to determine the values of both the section resistances, $M_{c,Rd}$, and the member resistances, $M_{b,Rd}$, under bending of these beams tested in Series SA, SB and SC, and it was highly desirable to examine structural adequacy and efficiency of the relevant design rules given in EN 1993-1-1 [17].

4.1 Section resistances under bending

In general, the moment resistances of fully restrained beams of S690 welded I-sections, $M_{c,Rd}$, were readily assessed according to Cl. 6.2.5. Hence, both the elastic and the plastic section resistances of Sections HSB1 to HSB6 were determined according to the measured dimensions and the measured yield strengths of their flanges and webs to give the section resistances of these sections under bending, $M_{c,Rd}$, as shown in Table 3. It should be noted that:

- Section HSB1 was classified as a Class 1 section, and its plastic section resistance was adopted.
- Both Sections HSB2 and HSB4 were classified as Class 2 sections, and hence, their plastic section resistances were adopted.
- Section HSB3 was classified as a Class 3 section, and its elastic section resistance was readily adopted.
- Both Sections HSB5 and HSB6 were classified as Effective Class 2 sections as permitted in Cl.5.5.2 [11] and 6.2.2.4, and hence, the plastic section resistances of their effective cross-sections are adopted. It should be noted that such a re-classification is not applicable to Section HSB3 because of its Class 3 flanges.

553

554 **4.2 Member resistances under bending**

555 According to EN 1993-1-1, partially restrained beams were expected to fail in lateral torsional
556 buckling, and the design rules given in Cl. 6.3.2 were readily applicable to determine the
557 member resistances to bending, $M_{b,Rd}$ or $\chi_{LT} M_{c,Rd}$, where χ_{LT} is the reduction factor for lateral
558 torsional buckling, and $M_{c,Rd}$ are the moment resistances of the cross-sections of the beams.

559

560 Based on the elastic critical moment resistances M_{cr} predicted with finite element models in
561 Section 3, the non-dimensionalized slenderness $\overline{\lambda}_{LT}$ for all the beams in Series SA, SB and SC
562 were obtained and presented in Tables 3b), 4b) and 5b) respectively. Through the use of Cl.
563 6.3.2.3 Lateral torsional buckling curves for rolled sections or equivalent welded sections and
564 Equation 6.57, Buckling Curve "*d*" was adopted according to EN 1993-1-12 [27]. The
565 buckling moment resistances $M_{b,Rd}$ of all the beams in Series SA, SB and SC were determined
566 accordingly, and the back analysis values of $M_{b,Rd}$ were presented in Tables 3b), 4b) and 5b)
567 respectively. It should be noted that all of these data were plotted onto the graph in Figure 17
568 together with various buckling curves for direct comparison.

569

570 It was shown that

571 • for all the beams in Series SA, their data were above the design curves in the region of $\overline{\lambda}_{LT}$
572 < 0.4, and hence, the moment resistances $M_{c,Rd}$ of these beams were significantly larger
573 than the design values of these effectively restrained beams; and
574 • similarly, for all the beams in Series SB and SC, their data were well above Buckling Curve
575 "*d*" in the region of $\overline{\lambda}_{LT} \geq 0.4$, and hence, the buckling moment resistances $M_{b,Rd}$ of these
576 beams were significantly larger than the design values of these partially restrained beams.

577

578 By establishing a model factor ρ_c as a ratio of the measured moment resistance M_{Rt} to the back
579 analysis value of the section resistance $M_{c,Rd}$ of all the beams in Series SA, it is shown in Table
580 3b) that the model factors ρ_c for the beams in Series SA range from 1.03 to 1.25 with an average
581 value at 1.10. Hence, the current design rules on section classification were demonstrated to
582 be valid when being extended to cover these beams of S690 welded I-sections.

583

Similarly, by establishing a model factor ρ_b as a ratio of the measured moment M_{Rt} to the back analysis value of the buckling moment resistance $M_{b,Rd}$ of all the beams in Series SB and SC, it is shown in Tables 4b) and 5b) that

a) for the beams in Series SB, the model factors ρ_b range from 1.15 to 1.21 with an average value at 1.18,
b) for the beams in Series SC, the model factors ρ_b range from 1.18 to 1.51 with an average value at 1.36, and
c) hence, the model factors ρ_b for the beams in both Series SB and SC range from 1.15 to 1.51 with an overall average value at 1.27.

Hence, the current design rules are shown to be readily applicable to unrestrained beams of S690 welded I-sections though the buckling moment resistances according to Buckling Curve "*d*" are found to be rather conservative, when compared with the measured values. This situation is very similar to those investigations [21, 22] on slender columns of S690 welded H-sections under compression. This is generally believed to be the results of reduced effects of welding-induced residual stresses in these S690 welded I-sections, when compared with those in S355 welded I-sections, because of increased yield strengths. Hence, it is highly desirable to adopt other curves, such as Buckling Curve "*c*" or Buckling Curve "*b*", for an improved structural efficiency of the current design rules.

5 Conclusions

In order to promote effective use of high strength steels in construction, it was important to examine the structural behaviour of partially restrained beams of high strength S690 welded I-sections against lateral torsional buckling. A systematic experimental investigation into the structural behaviour of a total of eighteen simply supported beams of high strength S690 welded I-sections with various restraint conditions was conducted, and these beams were demonstrated to behave essentially similarly to those beams of S355 I-sections. Key results of these beam tests were analysed to assess the validity of the current design rules given in EN 1993-1-1 when being extended to cover these beams. The following conclusions were found:

a) Effectively restrained beams

In Series SA, these beams of S690 welded I-sections were effectively restrained, and their section resistances under bending, $M_{c,Rd}$, were readily mobilized as follows:

1. The measured moment resistances, M_{Rt} , of those beams classified as both Class 1 and 2 sections were shown to be larger than their plastic moment resistances, $M_{pl,Rd}$, based on measured dimensions and yield strengths. For those sections classified as Class 3 sections, their measured moment resistances, M_{Rt} , were shown to be larger than the elastic moment resistances, $M_{el,Rd}$, of their cross-sections. Moreover, for those sections classified as Effective Class 2 sections, their measured moment resistances, M_{Rt} , were shown to be larger than the plastic moment resistances of their effective cross-sections, $M_{pl,Rd,eff}$.

2. Hence, the section classification rules given in EN 1993-1-1 were found to be readily applicable to those S690 welded I-sections, in particular, for the Class 2 sections and the Effective Class 2 sections.

b) Partially restrained beams undergoing lateral torsional buckling

In Series SB and SC, these beams of S690 welded I-sections were partially restrained, and lateral torsional buckling was critical in all of them. It should be noted that:

1. The measured moment resistances, M_{Rt} , of all the beams in both Series SB and SC were shown to be significantly larger than the back analysis values of the buckling moment resistances, $M_{b,Rd}$, based on measured dimensions and yield strengths.

2. Buckling Curve "*d*" in EN 1993-1-1 was found to give conservative buckling moment resistances for all the beams in both Series SB and SC. The model ratios M_{Rt} / $M_{b,Rd}$ were found to range from 1.15 to 1.51 with an overall average value at 1.27. This was generally believed to be the results of reduced effects of welding-induced residual stresses in these beams of S690 welded I-sections, when compared with those in S355 welded I-sections, because of increased yield strengths.

3. It was highly desirable to improve design efficiency of the design rules given in EN 1993-1 when being extended to cover lateral torsional buckling of partially restrained beams of S690 welded I-sections.

4. Through the use of the finite element modelling technique and a proper modelling of the lateral restraints to these beams, both the elastic critical moment resistance, M_{cr} , and the non-dimensionalized slenderness $\overline{\lambda}_{LT}$ of these beams were readily determined. Hence, the design methodology for beam buckling given in EN 1993-1-1 was considered to be highly effective.

c) Residual stresses

Through a proper control on the welding parameters and procedures during welding of these high strength S690 welded I-sections, the residual stresses of these beams were found to be very small as defined by the magnitudes of the surface residual stresses measured with the hole drilling method. Hence, these residual stresses of small magnitudes were an important condition for the observed performance of these beams undergoing lateral torsional buckling as demonstrated in the tests. It should be noted that any increase in the residual stresses due to a change in the welding parameters and procedures during welding of the beams may cause significant reductions in their buckling moment resistances.

It should be noted that all of these high strength S690 steel beams of welded I-sections should be fabricated with multi-pass welding, and the heat input energy is controlled not to exceed 1.3 kJ/mm in each pass. A tight limit for the fabrication tolerance on these beams at a ratio of a span over 1000 should be achieved. Moreover, the dimensions of both the flanges and the webs of these steel beams should be Class 1 to 3 sections according to the current rules for section classification to EN 1993-1-1. After calibration of the finite element models against test data, a comprehensive parametric study on lateral torsional buckling of high strength S690 welded I-sections with various geometrical dimensions will be carried out to provide more data. Then, based on both test and numerical data, a suitable buckling curve in accordance with the design methodology for beam buckling given in EN 1993-1-1 will be selected for improved structural efficiency. This will be reported in a separate paper.

Acknowledgement

The authors are grateful to the Research Grants Council of the Government of Hong Kong SAR for its financial support provided in Project Nos. PolyU 1526871/16E, 152231/17E and 152157/18E. The project leading to the publication of this paper was also partially funded by the Research Committee (Project No. RTZX and RJLY) of the Hong Kong Polytechnic University, and the Chinese National Engineering Research Centre for Steel Construction

(Hong Kong Branch) (Project No. 1-BBY3 & 6). It should be noted that the Research Centre was jointly funded by the Innovation and Technology Funds of the Government of Hong Kong SAR and the Hong Kong Polytechnic University. Special thanks go to the Nanjing Iron and Steel Co. Ltd. in Nanjing for supply of the high strength S690 steel plates, and the Pristine Steel Fabrication Co. Ltd. in Dongguan for fabrication of the S690 steel welded I-sections. All the experiments were carried out at the Structural Engineering Research Laboratory of Department of Civil and Environmental Engineering at the Hong Kong Polytechnic University, and supports from the technicians in testing of all the steel beams were highly appreciated.

References

1 BS EN 10025-6. (2004). Hot Rolled Products of Structural Steels – Part 6: Technical delivery conditions for flat products of high yield strength structural steels in the quenched and tempered condition. British Standards Institution.

2 Willms R. (2009). High strength steel for steel construction. Proceedings of Nordic Steel Construction Conference, pp597-604.

3 Timoshenko, S. P. and Gere, J. M. (1961). Theory of Elastic Stability.

4 Vlasov, V. Z. (1961). Thin-Walled Elastic Beams. Israel Program for Scientific Translations, Jerusalem.

5 Galambos, T. V. and Fukumoto, Y. (1963). Inelastic Lateral-torsional Buckling of Beam-columns. Fritz Engineering Laboratory, Lehigh University.

6 Fukumoto, Y., Fujiwara, M., and Watanabe, N. (1971). Inelastic lateral buckling tests on welded beams and girders. Proceedings of the Japanese Society of Civil Engineers, Paper 189: 39-51.

7 Nethercot D.A. and Rockey. K.C. (1971). A unified approach to the elastic lateral buckling of beams. The Structural Engineer, 321-329(49):7.

8 Nethercot, D. A. and Trahair, N. S. (1976). Inelastic lateral buckling of determinate beams. Journal of Structural Division, 102(ST4), 701-717.

9 Fukumoto, Y., Itoh, Y., and Kubo, M. (1980). Strength variation of laterally unsupported beams. Journal of Structural Division, ASCE, 106 (ST1): 165-181.

10 Pi, Y. L. and Trahair, N.S. (2000). Distortion and warping at beam supports. Journal of Structural Engineering 126: 1279–1287.

11 Dibley, J.E. (1969). Lateral Torsional Buckling of I-Sections in Grade 55 Steel. Proceedings of the Institution of Civil Engineers 43 (4). ICE Publishing: 599–627.

12 A. R. Kemp, M. P. Byfield and D. A. Nethercot, Effect of strain hardening on flexural properties of steel beams. The Structural Engineer. 80(8) (2002) 188-197.

13 Kerdal, D. and Nethercot, D (1984). Failure modes for castellated beams. Journal of Constructional Steel Research, 4(4): 295-315.

14 Trahair, N. S. (1993). Flexural-Torsional Buckling of Structures. CRC Press, Boca Raton, FL.

15 Bradford, M.A. (2000). Strength of compact steel beams with partial restraints. Journal of Constructional Steel Research 53: 183–200.

16 Trahair, N. S., Bradford, M. A., Nethercot, D. and Gardner, L. (2007). The Behaviour and Design of Steel Structures to EC3. CRC Press.

17 Kitipornchai, S, Wang, C. M. and Tarhair, N. S. (1986). Buckling of mono-symmetric I beams under moment gradient. Journal of Structural Engineering, ASCE, 112 (4): 781-799.

18 Jan V. and Stanb, T.C. (2017). FEM modelling of lateral-torsional buckling using shell and solid elements, Procedia Engineering 190: 464 – 471.

19 CEN. (2005). EN 1993-1-1: Design of steel structures. Part 1-1: General rules and rules for buildings. European Committee for Standardization.

20 Ho, H.C., Chung, K.F., Huang, M.X., Nethercot, D.A., Liu, X., Hao, J., Wang, G.D. and Tian, Z.H. (2020). Mechanical properties of high strength S690 steel welded sections through tensile tests on heat-treated coupons, Journal of Constructional Steel Research, 166: 105922.

21 Liu, X., Chung, K. F., Ho, H. C., Xiao, M., Hou, Z. X. and Nethercot, D. A. (2018). Mechanical behavior of high strength S690-QT steel welded sections with various heat input energy. Engineering Structures, 175: 245-256.

22 Liu, X. and Chung, K.F. (2018). Experimental and numerical investigation into temperature histories and residual stress distributions of high strength steel S690 welded H-sections, Engineering Structures, 165, 396-411.

23 Ma, T.Y., Liu, X., Hu, Y.F., Chung, K.F. and Li, G.Q. (2018). Structural behaviour of slender columns of high-strength Q690 steel welded H-sections under compression, Engineering Structures, 157, 75-85, February 2018.

24 Ma, T.Y., Hu, Y.F., Liu, X., Li, G.Q. and Chung, K.F. (2017). Experimental investigation into high strength Q690 steel welded H-sections under combined compression and bending. Journal of Constructional Steel Research, 138: 449-462.

25 Hu, Y.F., Chung, K.F., Ban, H.Y. and Nethercot, D.A. (2020). Investigations into residual stresses in S690 cold-formed circular hollow sections due to transverse bending and longitudinal welding. Engineering Structures 219: 110911.

26 Hu, Y.F., Chung, K.F., Ban, H.Y. and Nethercot, D.A. (2021). Structural behaviour of T-joints between high strength S690 steel cold-formed circular hollow sections. Journal of Constructional Steel Research (accepted for publication).

27 BS EN ISO 6892-1 (2009). Metallic materials – Tensile testing: Part 1: Method of test at ambient temperature, British Standards Institution.

28 Ho, H.C., Chung, K.F., Liu, X., Xiao, M. and Nethercot, D.A. (2019). Modelling tensile tests on high strength S690 steel materials undergoing large deformations. Engineering Structures, 192: 305-322.

29 CEN. (2007). BS EN 1993-1-12: Design of steel structures. Part 1-12: Additional rules for the extension of EN 1993 up to steel grades S700. European Committee for Standardization.

30 American Welding Society. (2005). Specification for low-alloy steel electrodes and rods for gas shielded arc welding. Structural Welding Code – Steel. Miami, United States.

31 ASTM E837 (2020). Standard Test Method for Determining Residual Stresses by the Hole-Drilling Strain-Gage Method. American Standards and Testing Methods.

32 Wang, K. (2018). Study on structural behaviour of high strength steel S690 welded H- and I-sections. Doctoral dissertation, The Hong Kong Polytechnic University.

33 European Convention for Constructional Steelworks (1976). Manual on Stability of Steel Structures, 2nd Edition. Committee 8: Stability. Brussels.

34 Systemes, D. (2014). ABAQUS 6.14 Documentation. *Providence, RI*.

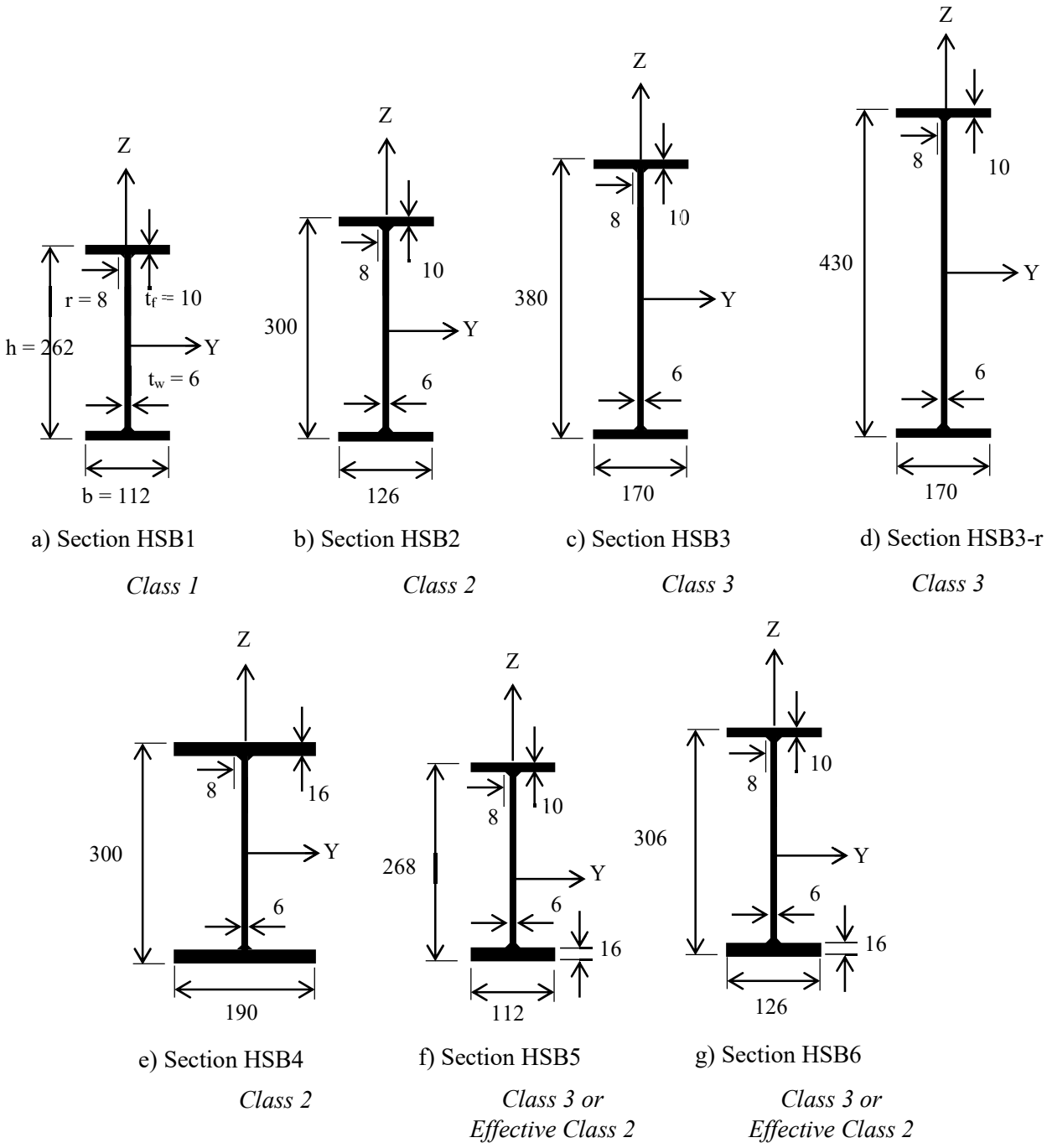

Figure 1 Cross-sectional dimensions of high strength S690 welded I-sections

Note: All these sections are tested in Series SA, SB and SC except that

i) Section HSB3 is tested in Series SA, and

ii) Section HSB3-r is tested in Series SB and SC.

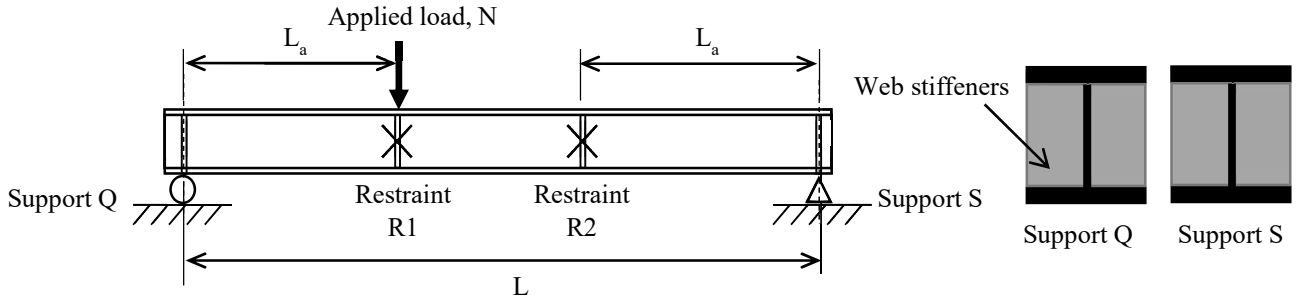

a) Series SA

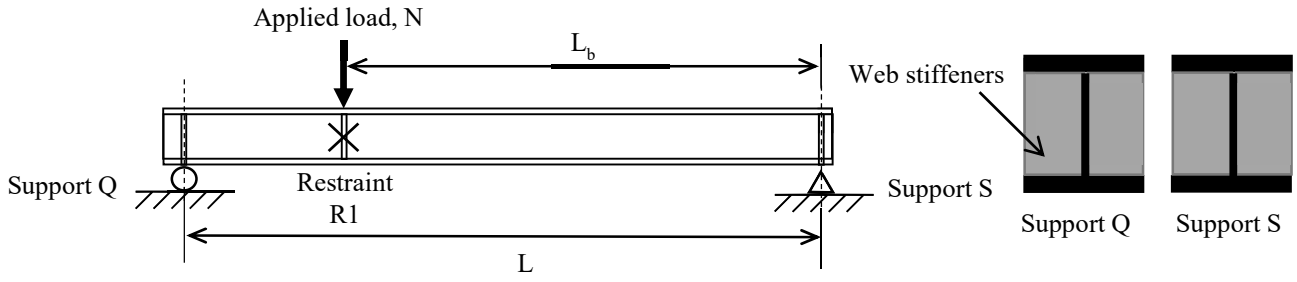

b) Series SB

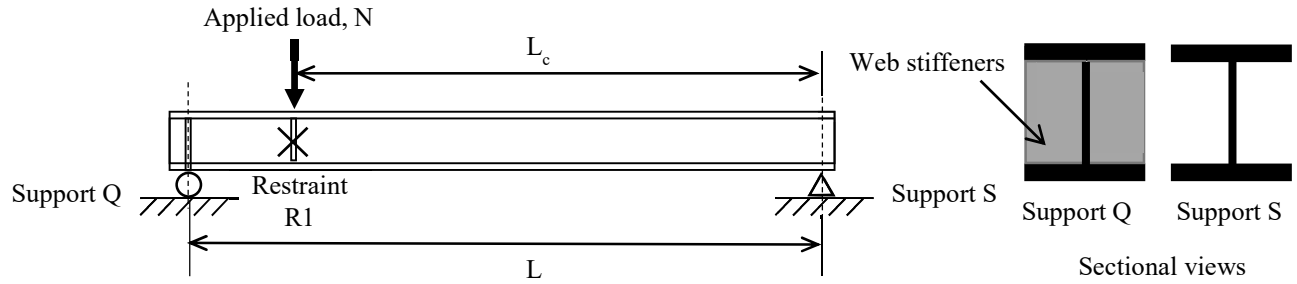

c) Series SC

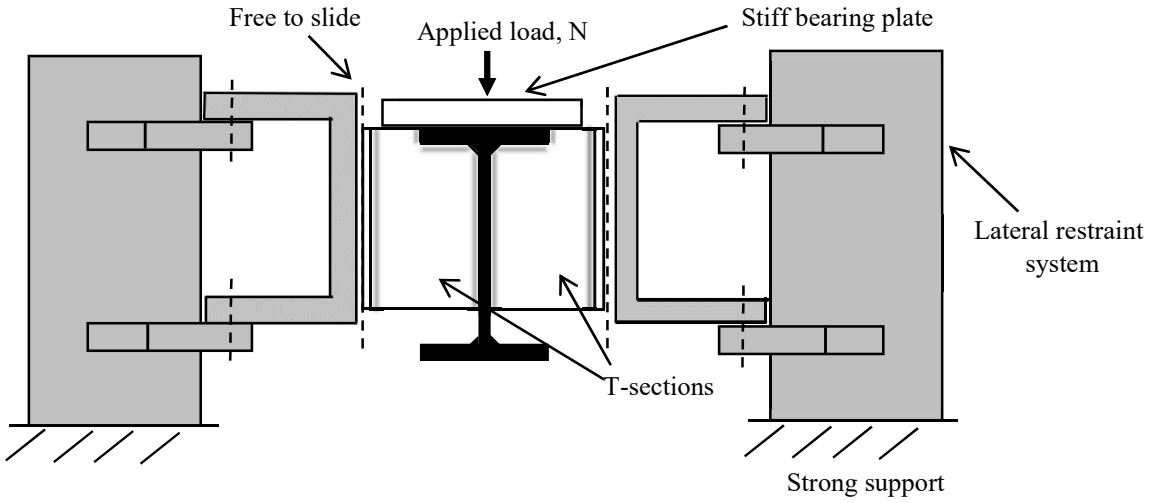

d) Stiff lateral restraint system

Figure 2 Loading and restraint conditions

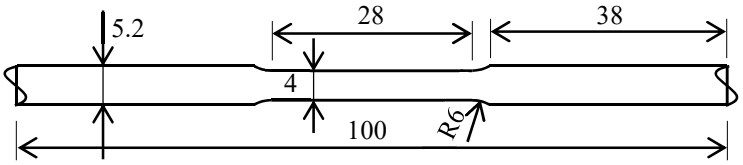

Standard coupon from 6 mm thick steel plates

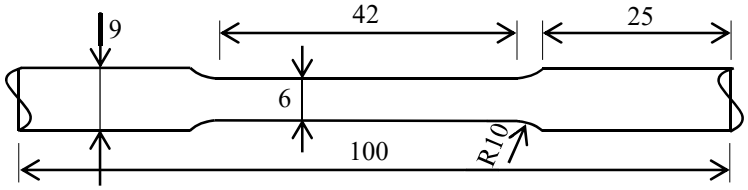

Standard coupon from 10 mm and 16 mm thick steel plates

a) Dimensions of coupons

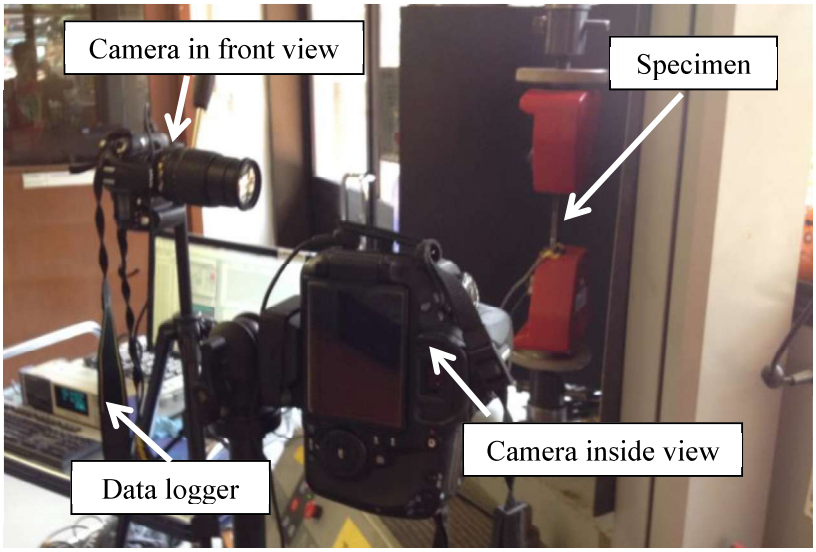

b) Typical coupon tests

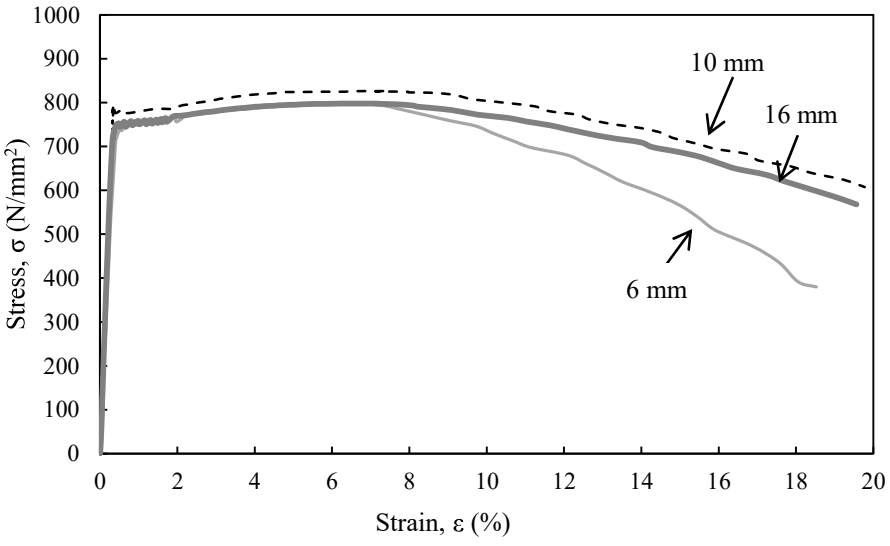

c) Measured stress-strain curves of S690 steels

Figure 3 Standard coupons tests for S690 steels

Figure 4 Welding of an I section – GMAW

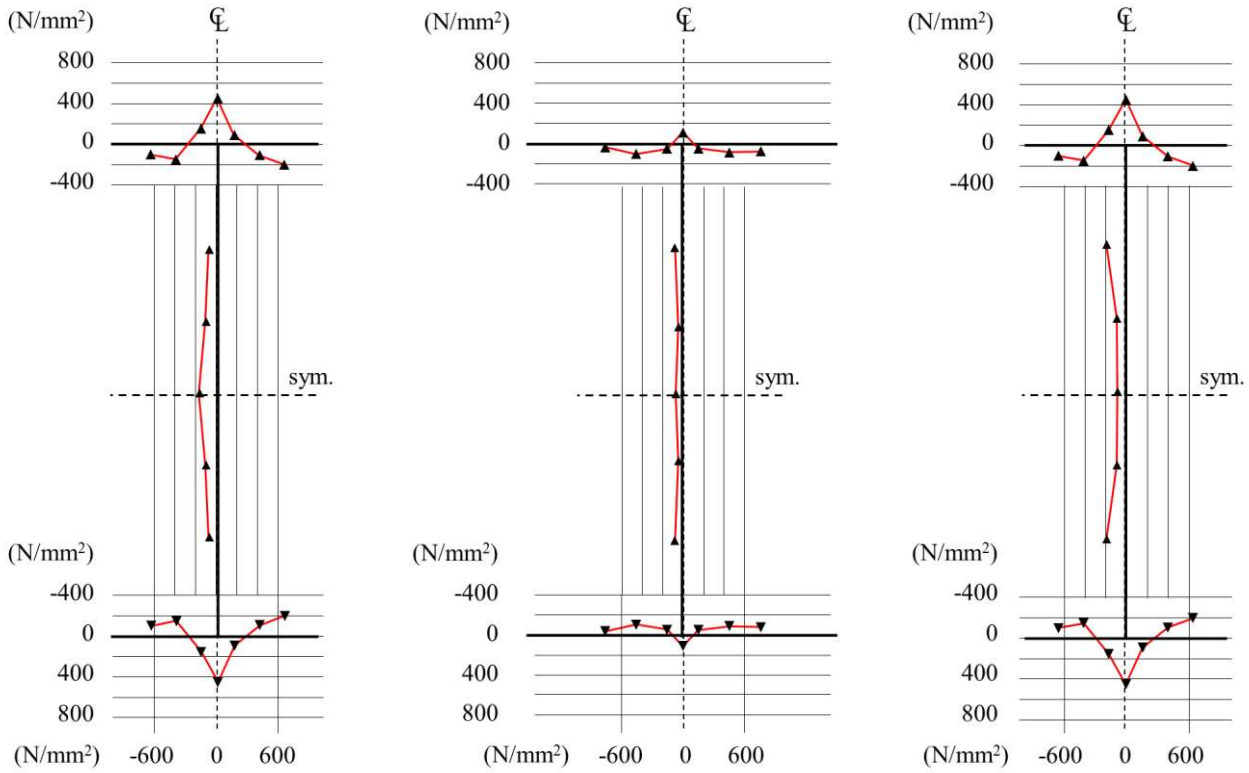

a) Section HSB2 b) Section HSB4 c) Section HSB6

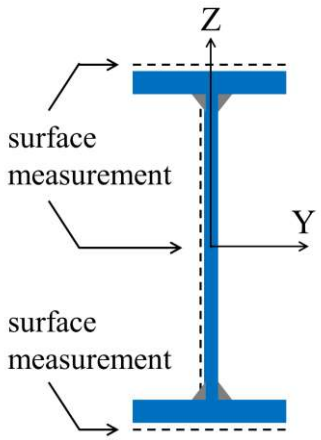

Figure 5 Typical measured surface residual stress distributions of welded I-sections

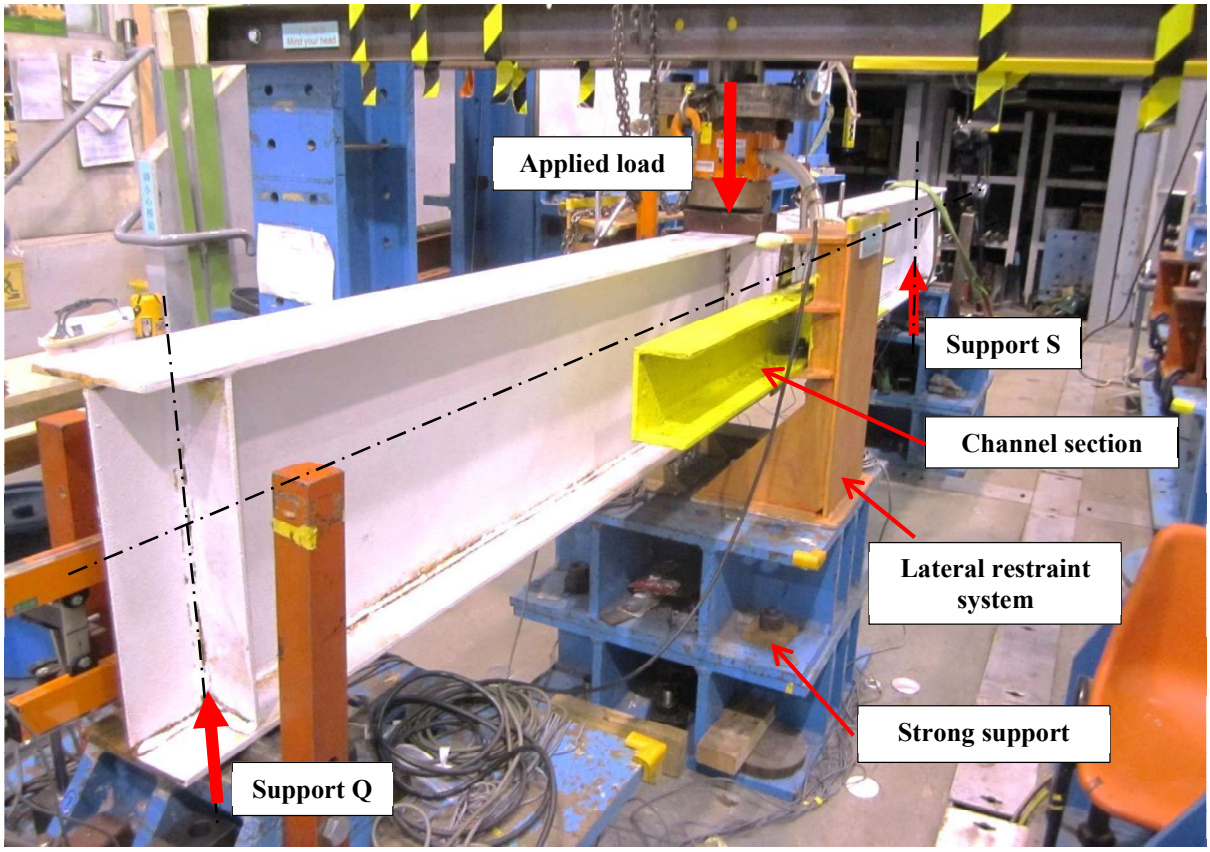

a) Overall view

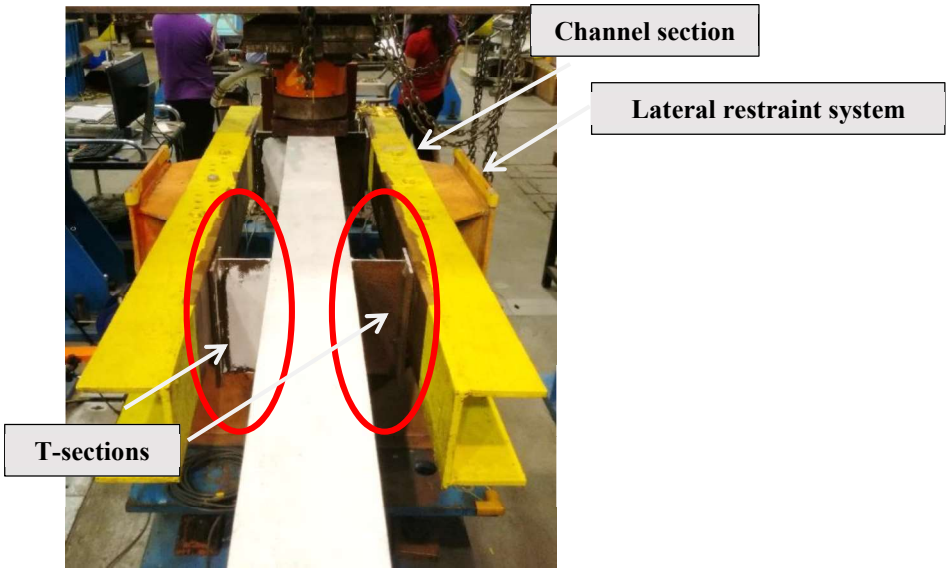

b) Longitudinal view

Figure 6 Typical test set-up

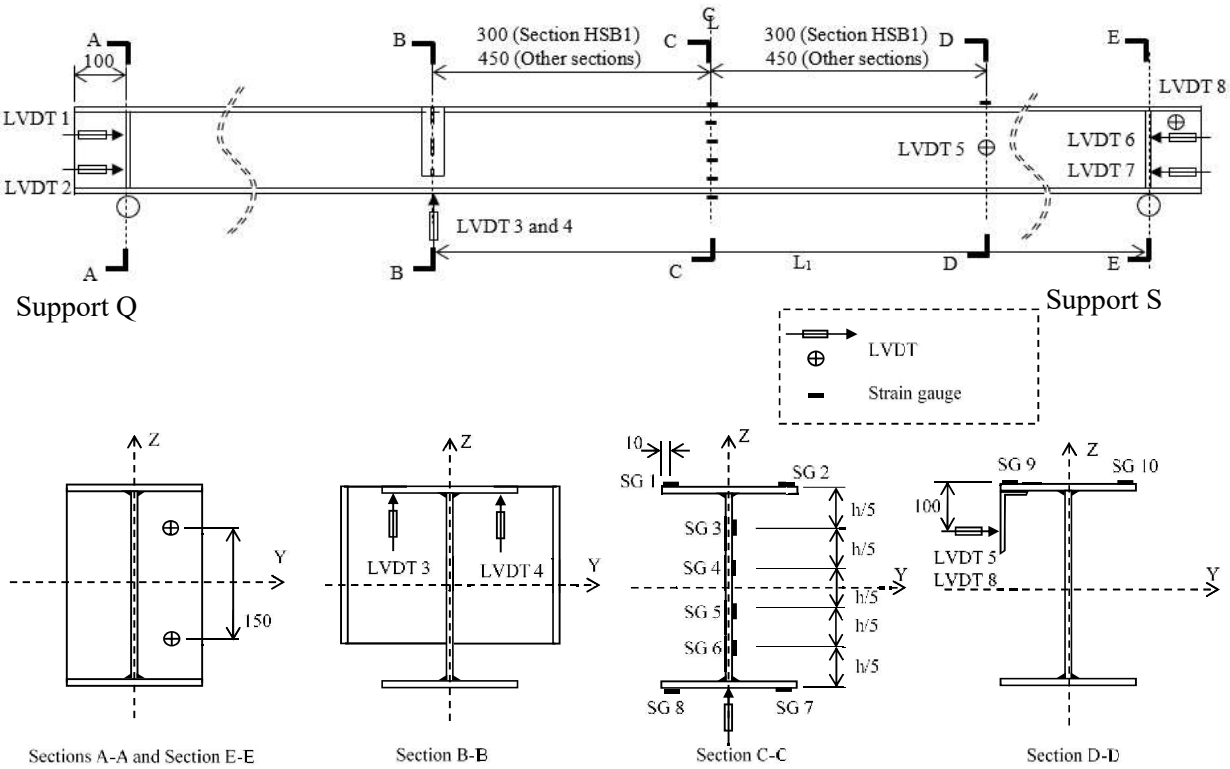

Figure 7 Typical instrumentation

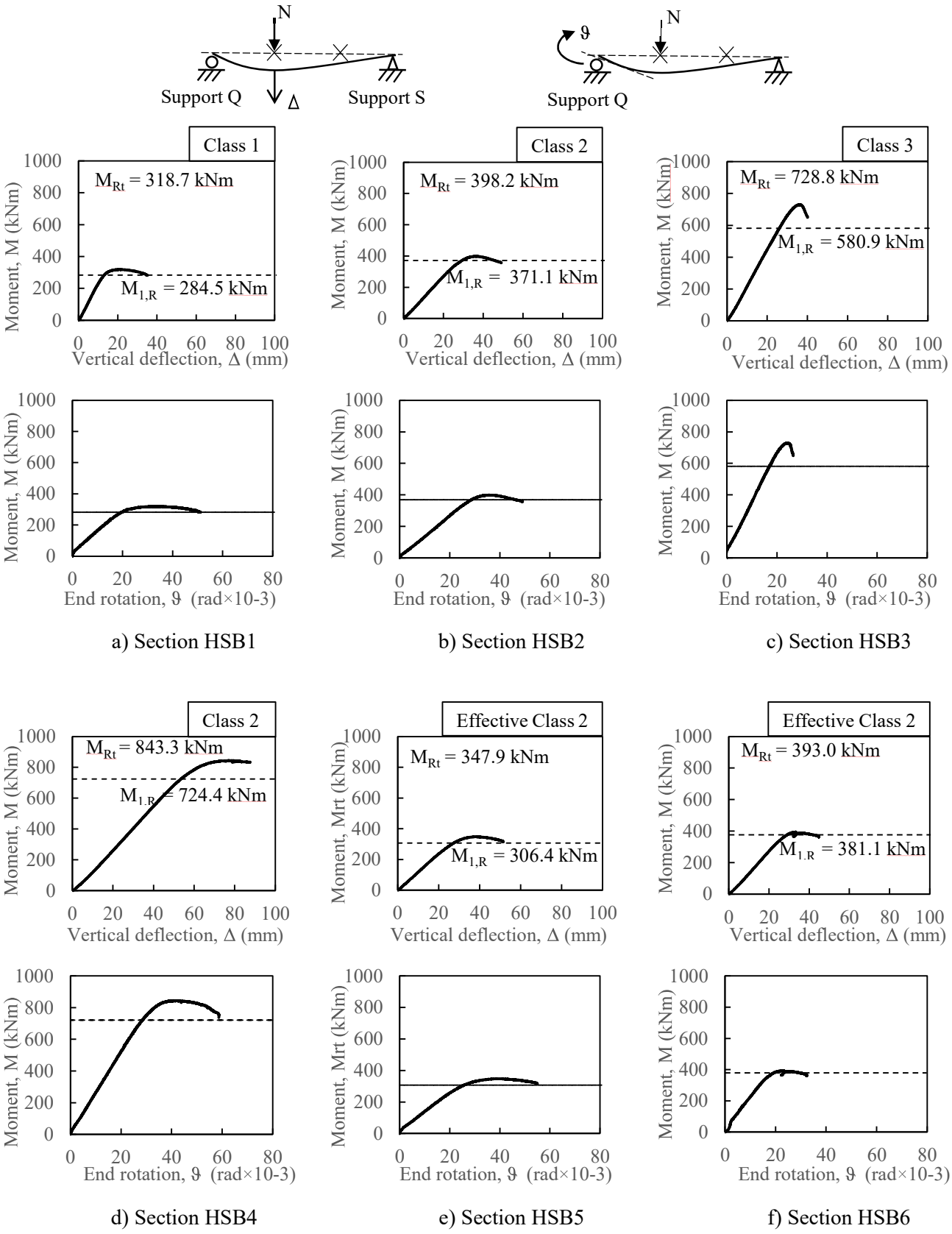

Figure 8 Load-deformation curves of Series SA

Note: $M_{1,R}$ are the back analysis values of the moment resistances of the beams in Series SA for member resistances.

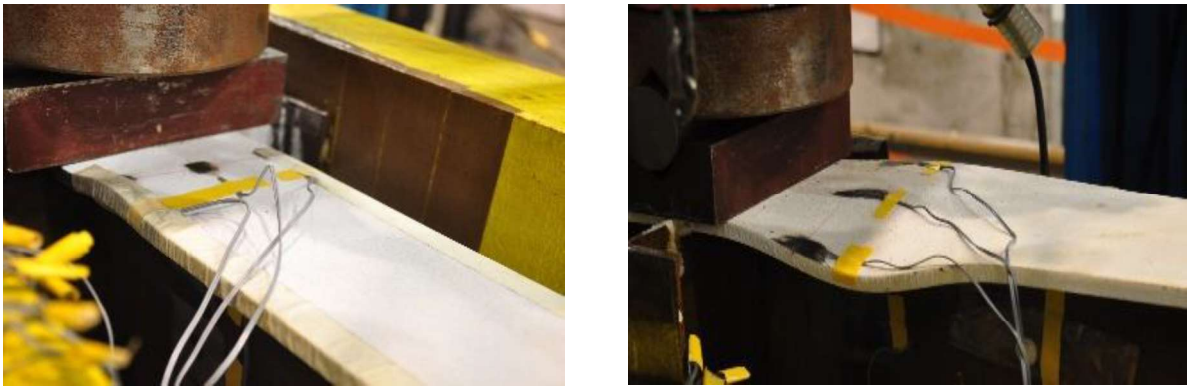

a) Section HSB2 in Series SA b) Section HSB3 in Series SA

Figure 9 Apparent local plate buckling in top flanges of the sections after test

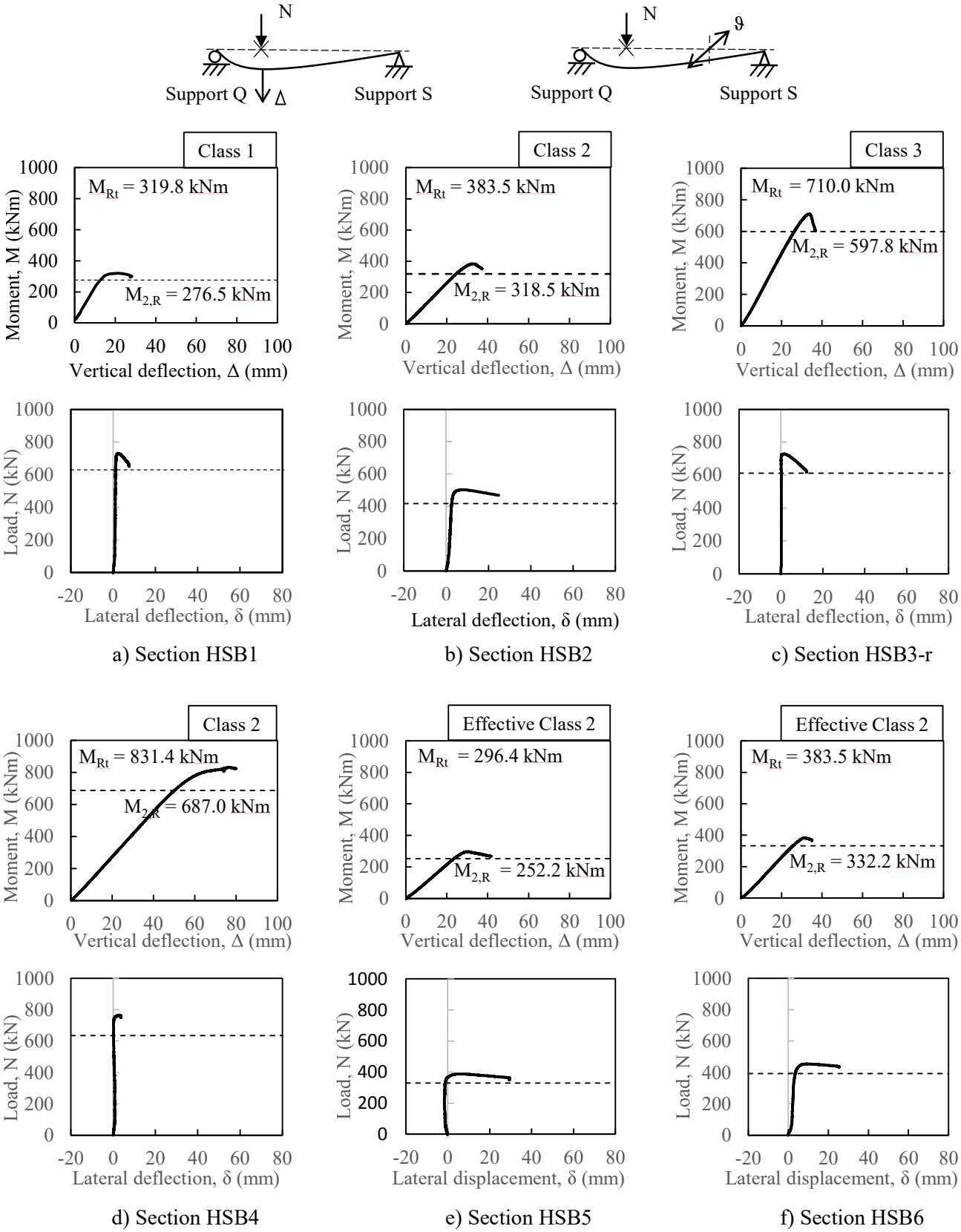

Figure 10 Load-deformation curves of beams in Series SB

Note: $M_{2,R}$ are the back analysis values of the moment resistances of the beams in Series SB for member resistances.

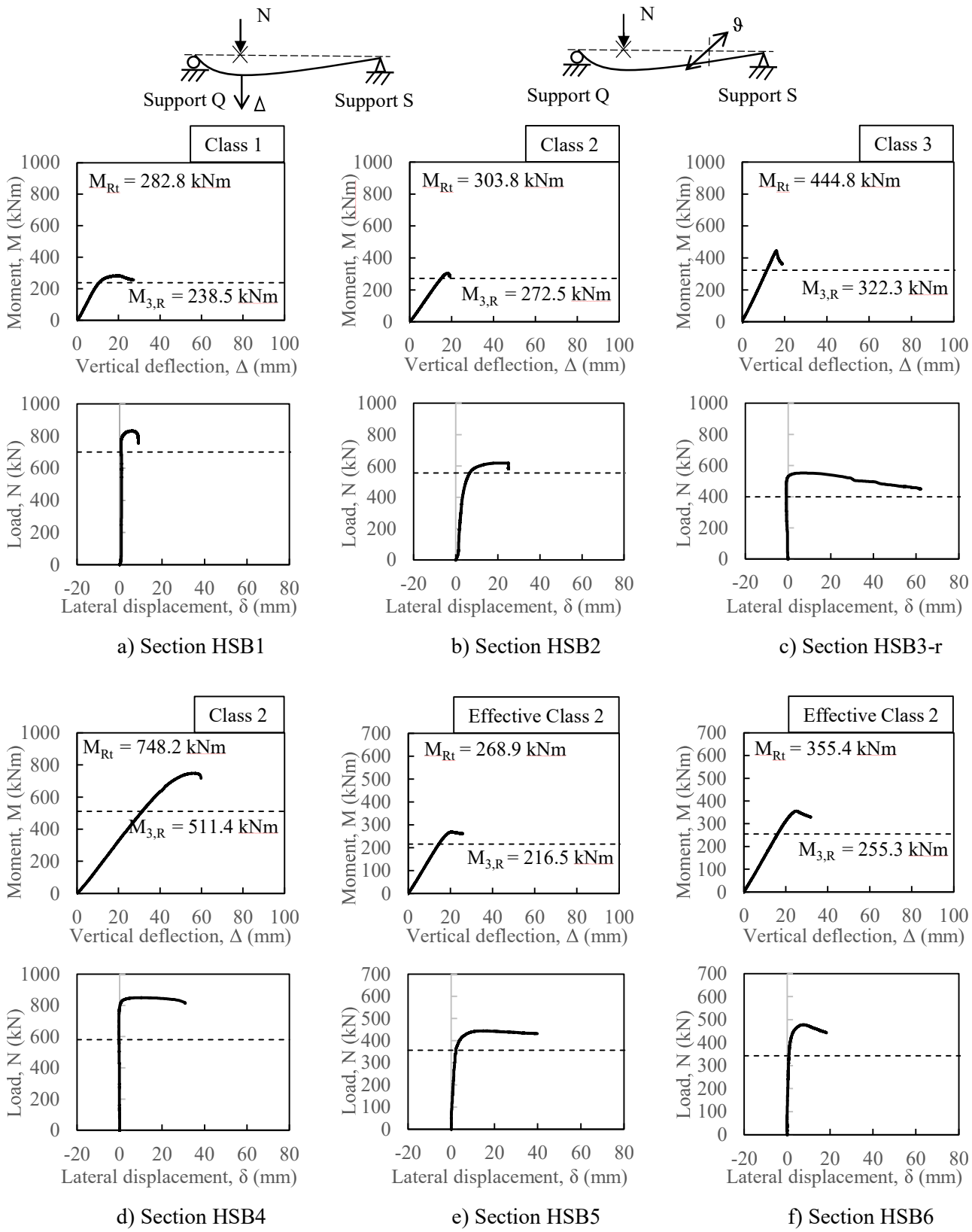

a) Section HSB1 b) Section HSB2 c) Section HSB3-r

d) Section HSB4 e) Section HSB5 f) Section HSB6

Figure 11 Load deformation curves of Series SC

Note: $M_{3,R}$ are the back analysis values of the moment resistances of the beams in Series SC for member resistances.

a) Section HSB2 in Series SB

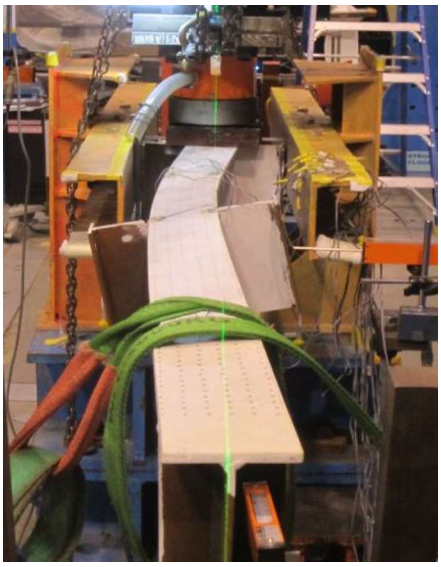

b) Section HSB5 in Series SB

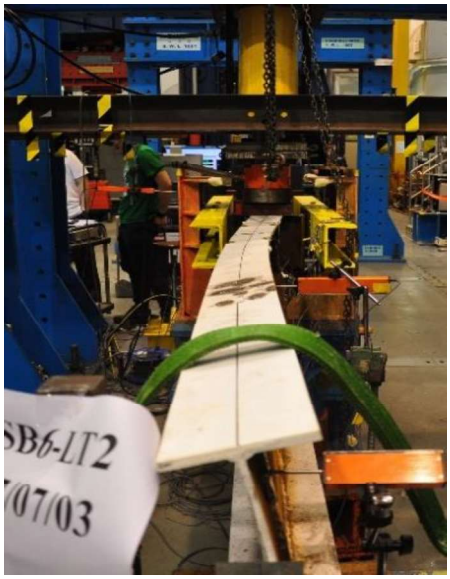

c) Section HSB6 in Series SC

d) Section HSB2 in Series SC

Note: (a, b) Lateral torsional buckling of beams, (c, d) Laterial torsional buckling beams with significant cross sectional distorion in unstiffened end supports.

Figure 12 Observed deformations of partially restrained beams

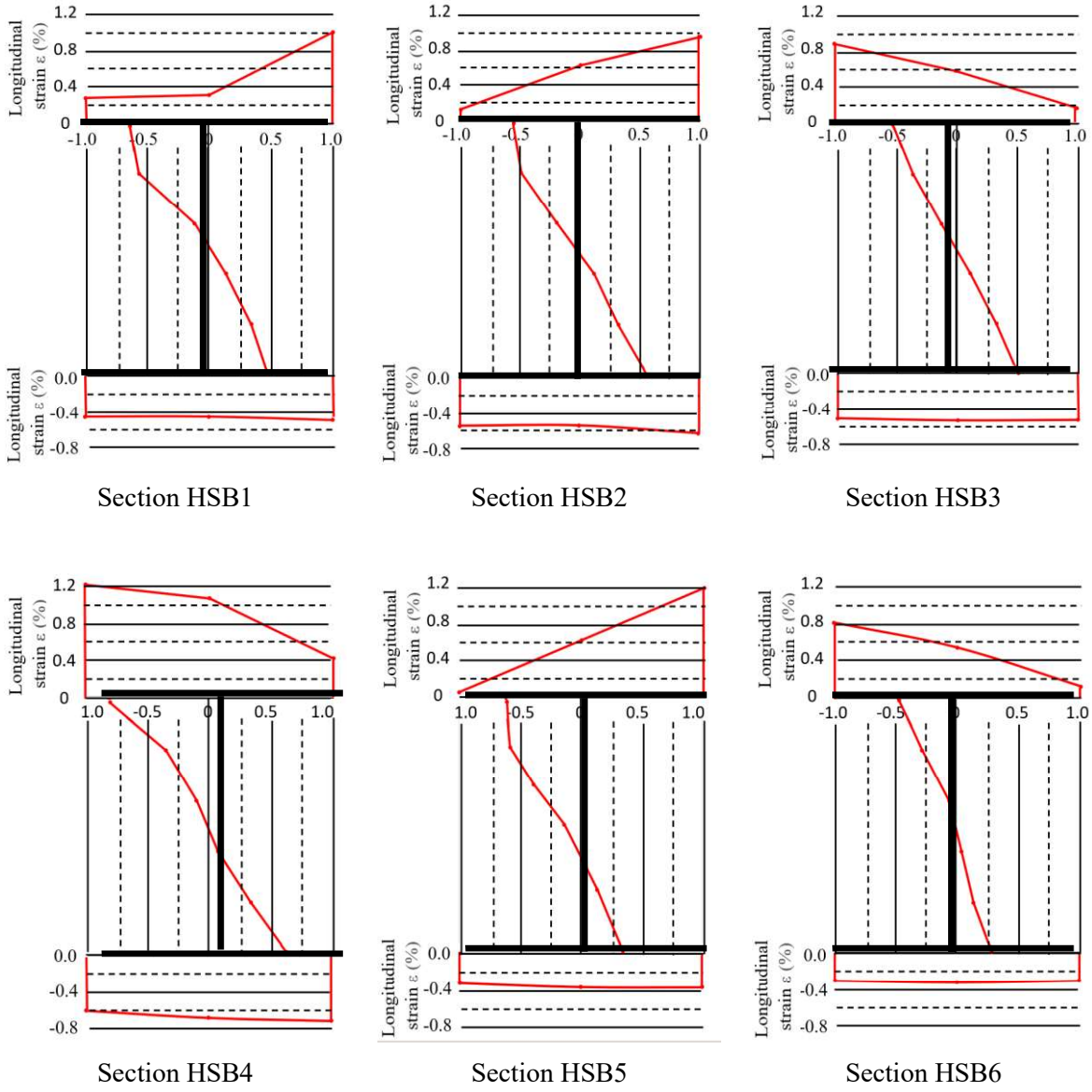

Figure 13 Measured strains of various sections at failure – Series SA

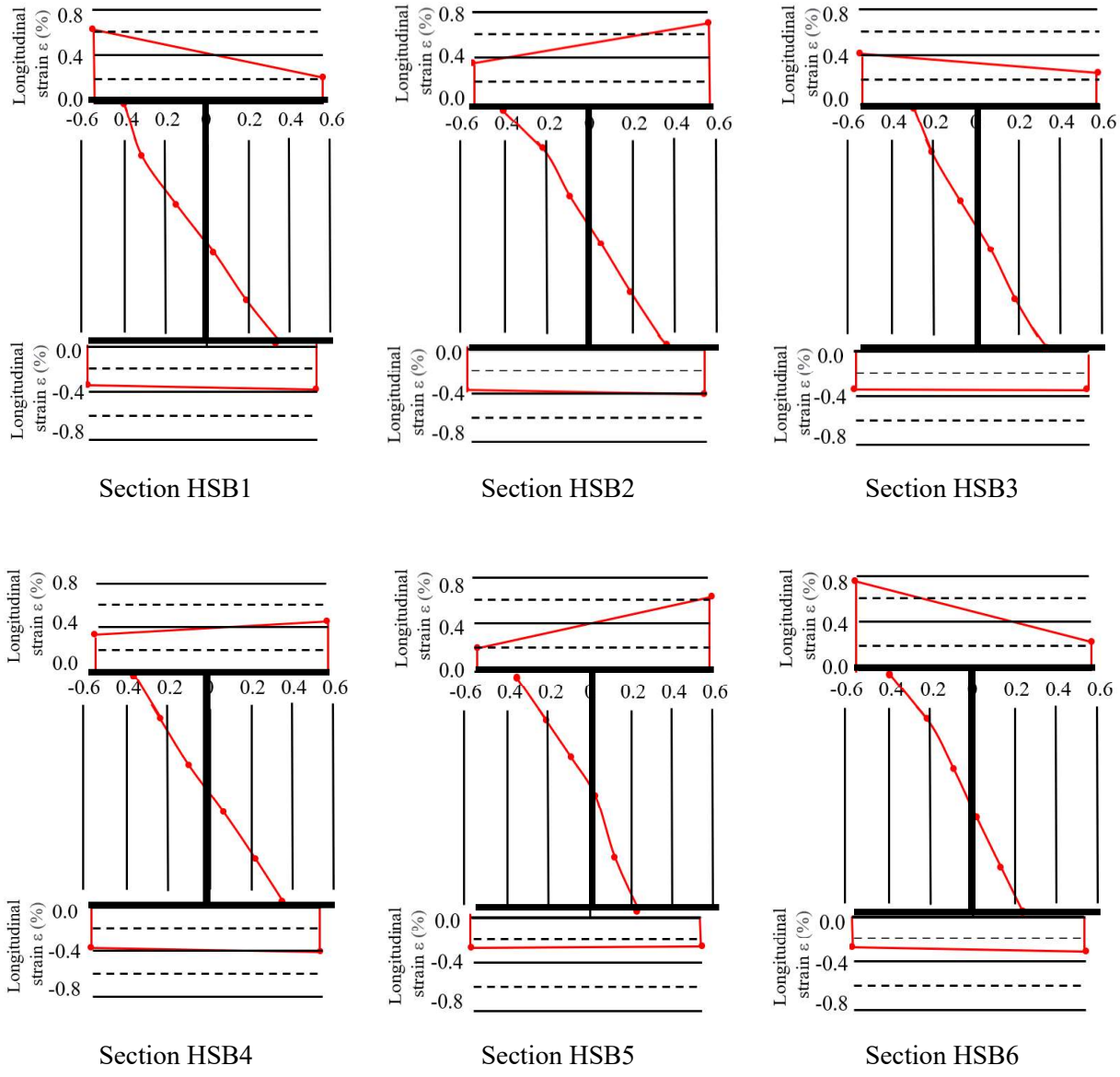

Figure 14 Measured strains of various sections at failure – Series SB

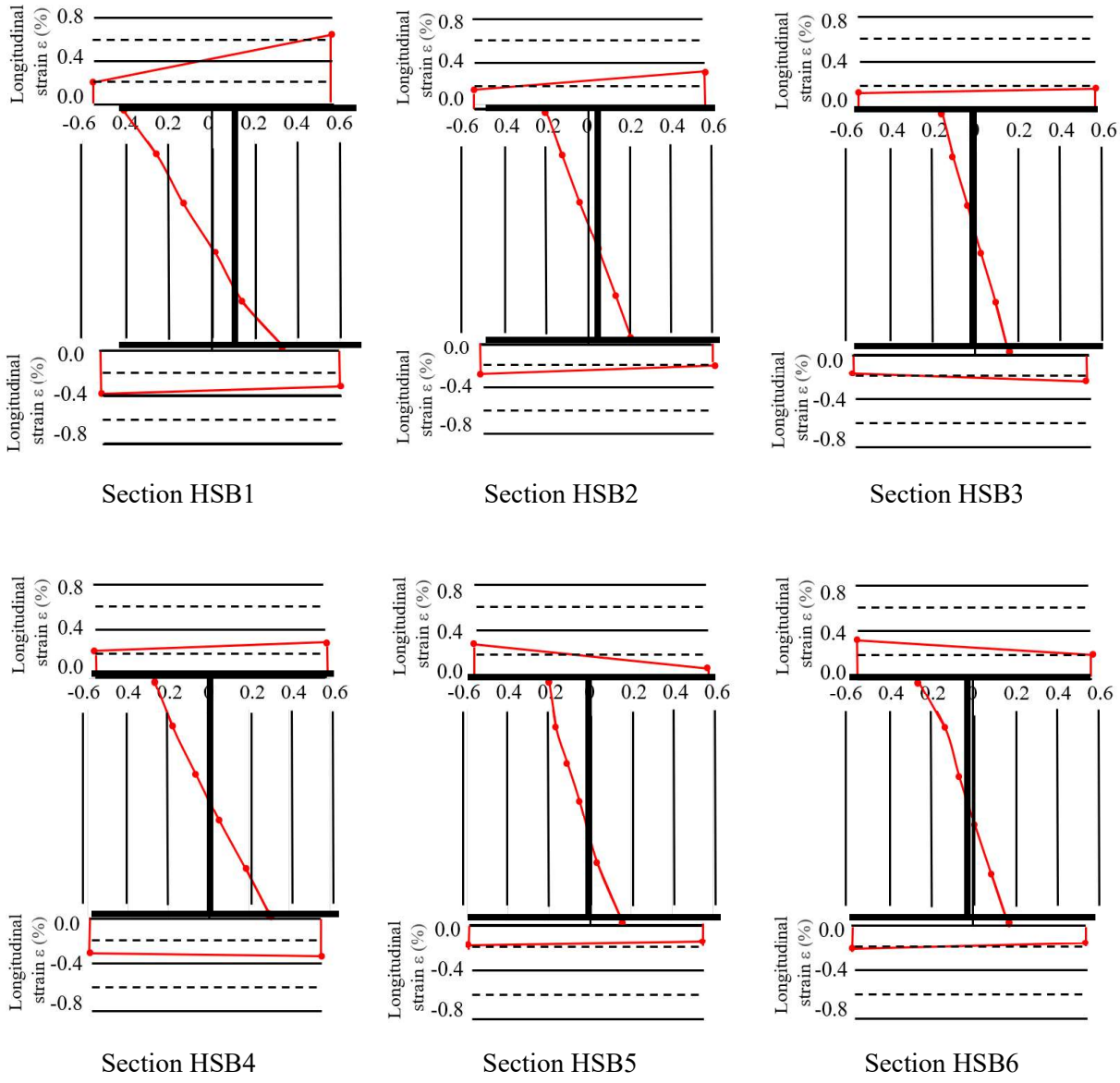

Figure 15 Measured strains of various sections at failure – Series SC

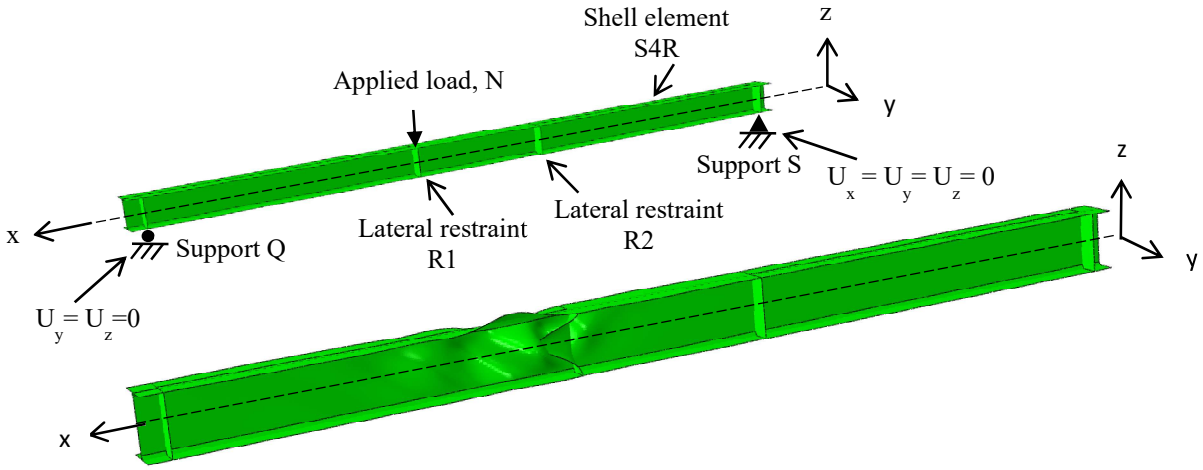

a) Typical eigenmode of a beam in Series SA

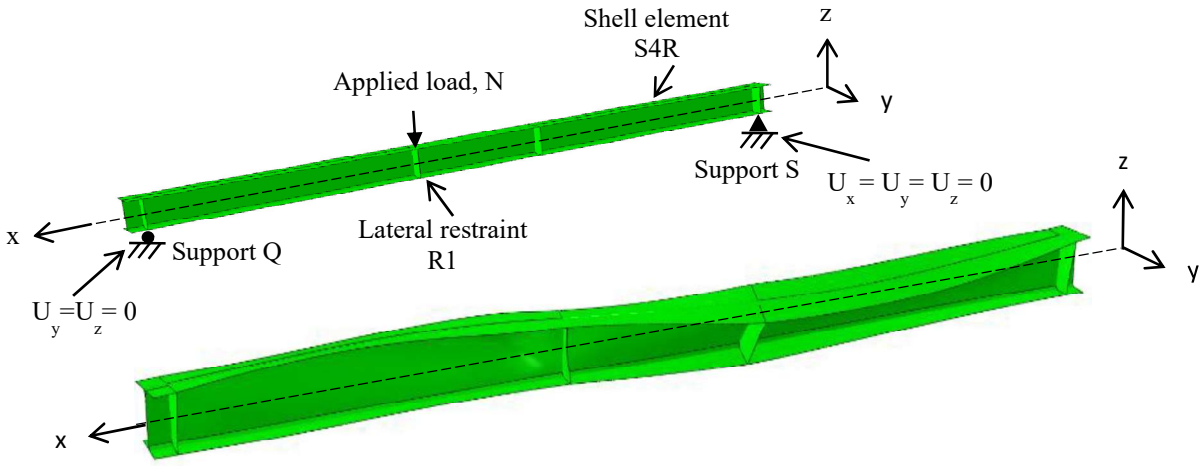

b) Typical eigenmode of a beam in Series SB

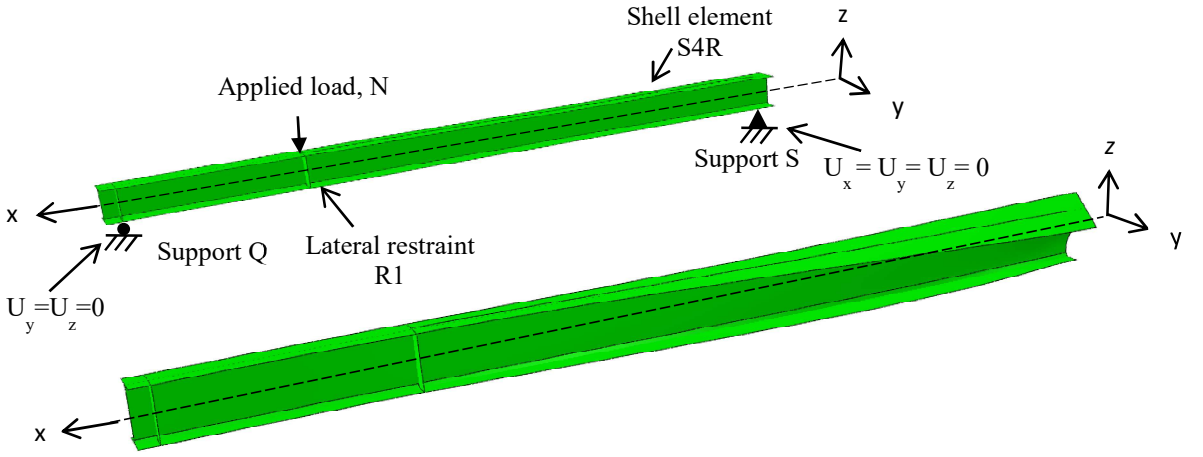

c) Typical eigenmode of a beam in Series SC

Figure 16 Typical finite element models for beams in various series

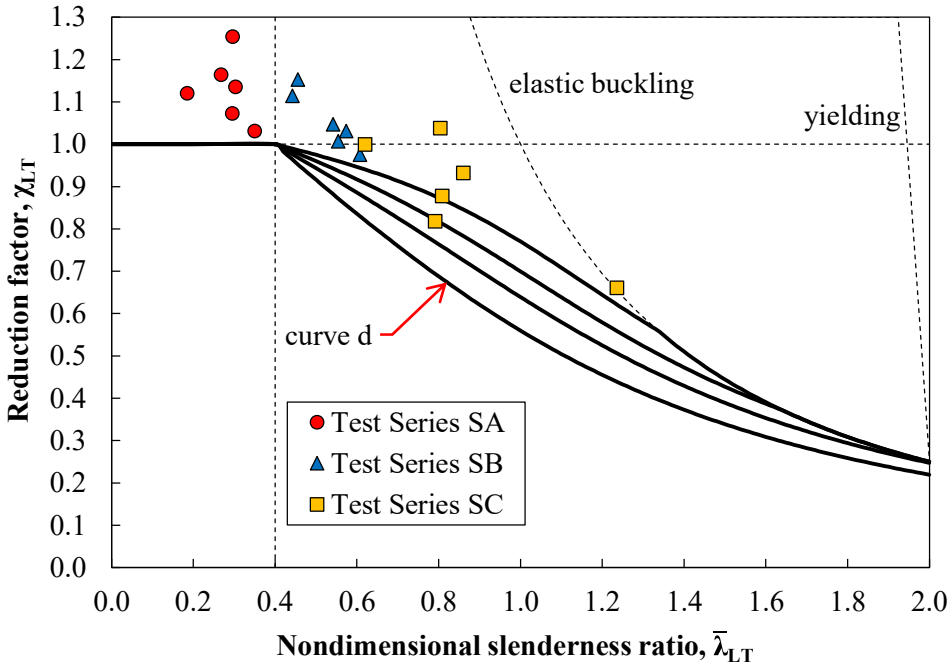

Figure 17 Reduction factors for beam buckling in EN 1993-1-1

Table 1 Coupon test results

Plate thickness (mm)	Yield Strength f_{ya} (N/mm^2)	Tensile strength f_u (N/mm^2)	Young's modulus E (kN/mm^2)	Strain at tensile strength ε_u (%)	Elongation at fracture ε_L (%)
6	720	843	211	6.41	19.1
10	784	874	206	7.42	19.8
16	745	832	216	6.62	19.6

Table 2 Measured welded parameters

Welding method: GMAW Electrode: GM110	Number of welding passes	Welding parameters			
		Voltage U (V)	Current I (A)	Speed v (mm/s)	Line heat energy input q (kJ/mm)
6 to 10 mm	1	28	225	5.3	1.01
6 to 16 mm	2	28	225	4.2	1.28
10 to 16 mm	3	28	225	4.8	1.12

Table 3 Test programme and results of Series SA

a) Measured dimensions and section parameters

Beam	Measured dimensions						Section parameters					
	h	b	t_f	t_w	Total span L	Shear span L_a	Section classification			$M_{c,Rd}$	M_{cr}	$\bar{\lambda}_{LT}$
	(mm)	(mm)	(mm)	(mm)	(mm)	(mm)	Flange	Web	Overall	(kNm)	(kNm)	
HSB1	262	112	10.0	6.0	1,940	670	Class 1	Class 1	Class 1	284.5	8313.4	0.19
HSB2	300	126	10.0	6.0	3,300	1,200	Class 2	Class 2	Class 2	371.1	4264.8	0.29
HSB3	380	170	10.1	6.0	4,100	1,600	Class 3	Class 3	Class 3	580.9	6630.3	0.30
HSB4	300	190	16.1	6.0	4,500	1,800	Class 2	Class 2	Class 2	724.4	10086.5	0.27
HSB5	268	112	TF: 10.0 BF: 16.0	6.0	3,300	1,200	Class 1	Class 3	#Class 2[1)]	306.4	3337.9	0.30
HSB6	306	126	TF: 10.0 BF: 16.0	6.0	3,600	1,350	Class 2	Class 3	#Class 2[1)]	381.1	3111.0	0.35

b) Design parameters and measured resistances

Beam	Parameters			Failure mode[2)]	Measured resistances		
	$\bar{\lambda}_{LT}$	χ_{LT}	$M_{c,Rd}$[4)] (kNm)		N_{Rt} (kN)	M_{Rt} (kNm)	$\frac{M_{Rt}}{M_{c,Rd}}$
HSB1	0.19	1.000	284.5	YS	726.6	318.7	1.12
HSB2	0.29	1.000	371.1	YS	521.5	398.2	1.07
HSB3	0.30	1.000	580.9	YS	747.0	728.8	1.25
HSB4	0.27	1.000	724.4	YS	780.8	843.3	1.16
HSB5	0.30	1.000	306.4	YS	455.6	347.9	1.14
HSB6	0.35	1.000	381.1	LTB[3)]	465.8	393.0	1.03
						Average:	1.10

Notes:

1) "#Class 2" denotes an effective Class 2 section.

2) "YS" denotes a failure mode due to yielding of the section.
"LTB" denotes a failure mode due to lateral torsional buckling of the member.

3) Section HSB6 was found to fail unexpectedly in LTB because of a local failure in the base of the lateral restraint system.

4) $M_{c,Rd}$ are the back analysis values of the section resistances of the sections based on measured dimensions and yield strengths.

Table 4 Test programme and results of Series SB

a) Measured dimensions, section parameters and design moments

Beam	Measured dimensions						Section parameters					
	h	b	t_f	t_w	Total span L	Shear span L_b	Section classification			$M_{c,Rd}$	M_{cr}	$\bar{\lambda}_{LT}$
	(mm)	(mm)	(mm)	(mm)	(mm)	(mm)	Flange	Web	Overall	(kNm)	(kNm)	
HSB1	262.0	112.2	10.1	6.0	1,940	1,270	Class 1	Class 1	Class 1	286.9	1464.8	0.44
HSB2	300.0	126.3	10.0	6.0	3,300	2,100	Class 2	Class 2	Class 2	371.8	1130.0	0.57
HSB3-r	430.0	170.1	10.1	6.0	4,100	2,500	Class 3	Class 3	Class 3	677.9	2307.7	0.54
HSB4	300.0	190.1	16.0	6.0	4,500	2,700	Class 2	Class 2	Class 2	721.1	3473.3	0.46
HSB5	268.0	111.9	TF: 9.9 BF: 16.0	6.0	3,300	2,100	Class 1	Class 3	#Class 2[1)]	303.8	823.4	0.61
HSB6	306.0	125.9	TF: 10.0 BF: 16.0	6.0	3,600	2,250	Class 2	Class 3	#Class 2[1)]	380.9	1240.9	0.55

b) Design parameters and measured resistances

Beam	Parameters				Failure mode[2)]	Measured resistances			
	$\bar{\lambda}_{LT}$	χ_{LT}	$M_{c,Rd}$[3)] (kNm)	$M_{b,Rd}$[4)] (kNm)		N_{Rt} (kN)	M_{Rt} (kNm)	$\frac{M_{Rt}}{M_{c,Rd}}$	$\frac{M_{Rt}}{M_{b,Rd}}$
HSB1	0.44	0.964	286.9	276.5	LTB	729.0	319.7	1.11	1.16
HSB2	0.57	0.857	371.8	318.5	LTB	502.3	383.6	1.03	1.20
HSB3-r	0.54	0.882	677.9	597.8	LTB	727.8	710.0	1.05	1.19
HSB4	0.46	0.953	721.1	687.0	LTB	769.9	831.5	1.15	1.21
HSB5	0.61	0.830	303.8	252.2	LTB	388.1	296.4	0.98	1.18
HSB6	0.55	0.872	380.9	332.2	LTB	454.5	383.5	1.01	1.15
								Average:	***1.18***

Notes:

1) "#Class 2" denotes an effective Class 2 section.
2) "LTB" denotes a failure mode due to lateral torsional buckling of the member.
3) $M_{c,Rd}$ are the back analysis values of the section resistances of the sections based on measured dimensions and yield strengths.
4) $M_{b,Rd}$ are the back analysis values of the member resistances of the members based on measured dimensions and yield strengths, determined with "Curve d" in EN 1993-1-1.

Table 5 Test programme and results of Series SC

a) Measured dimensions and section parameters

Beam	Measured dimensions						Section parameters					
	h (mm)	b (mm)	t_f (mm)	t_w (mm)	Total span L (mm)	Shear span L_c (mm)	Section classification: Flange	Web	Overall	$M_{c,Rd}$ (kNm)	M_{cr} (kNm)	$\bar{\lambda}_{LT}$
HSB1	262.0	112.2	9.9	6.0	1,940	1,500	Class 1	Class 1	Class 1	282.9	735.0	0.62
HSB2	300.0	126.1	10.0	6.0	3,300	2,700	Class 2	Class 2	Class 2	371.4	362.0	0.79
HSB3-r	430.0	170.1	10.0	6.0	4,100	3,000	Class 3	Class 3	Class 3	672.8	496.3	1.24
HSB4	300.0	190.1	16.0	6.0	4,500	3,300	Class 2	Class 2	Class 2	721.1	2690.0	0.80
HSB5	268.0	111.9	TF: 10.0 BF: 16.0	6.0	3,300	2,500	Class 1	Class 3	#Class 2[1)]	306.2	413.0	0.81
HSB6	306.0	126.1	TF: 10.0 BF: 16.0	6.0	3,600	2,550	Class 2	Class 3	#Class 2[1)]	381.3	458.0	0.86

b) Design parameters and measured resistances

Beam	Parameters				Failure mode[2)]	Measured resistances			
	$\bar{\lambda}_{LT}$	χ_{LT}	$M_{c,Rd}$[3)] (kNm)	$M_{b,Rd}$[4)] (kNm)		N_{Rt} (kN)	M_{Rt} (kNm)	$\frac{M_{Rt}}{M_{c,Rd}}$	$\frac{M_{Rt}}{M_{b,Rd}}$
HSB1	0.62	0.820	282.9	232.1	LTB	831.2	282.8	1.00	1.22
HSB2	0.79	0.694	371.4	257.7	LTB	618.9	303.8	0.82	1.18
HSB3-r	1.24	0.439	672.8	295.5	LTB	552.6	444.8	0.66	1.51
HSB4	0.80	0.685	721.1	494.1	LTB	850.4	748.4	1.04	1.51
HSB5	0.81	0.682	306.2	208.9	LTB	443.7	268.9	0.88	1.29
HSB6	0.86	0.647	381.3	246.7	LTB	477.8	355.4	0.93	1.44
								Average:	***1.36***

Notes:

1) "#Class 2" denotes an effective Class 2 section.
2) "LTB" denotes a failure mode due to lateral torsional buckling of the member.
3) $M_{c,Rd}$ are the back analysis values of the section resistances of the sections based on measured dimensions and yield strengths.
4) $M_{b,Rd}$ are the back analysis values of the member resistances of the members based on measured dimensions and yield strengths, determined with "Curve d" in EN 1993-1-1.